

1 **RESEARCH ARTICLE**

2 **Transcriptional Regulation of Arabidopsis Polycomb Repressive**
3 **Complex 2 Coordinates Cell Type Proliferation and Differentiation**

4
5 **Miguel de Lucas^{1*}, Li Pu¹, Gina Turco¹, Allison Gaudinier¹, Ana Karina Morao²,**
6 **Hirofumi Harashima³, Dahae Kim¹, Mily Ron¹, Keiko Sugimoto³, Francois Roudier²,**
7 **Siobhan M. Brady¹**

8
9 ¹Department of Plant Biology and Genome Center, University of California, Davis, Davis,
10 CA 95616, USA

11 ²Institut de Biologie de l'Ecole Normale Supérieure (IBENS), Centre National de la
12 Recherche Scientifique (CNRS) Unité Mixte de Recherche (UMR) 8197 and Institut
13 National de la Santé et de la Recherche Médicale (INSERM) U1024, Paris, France.

14 ³RIKEN Center for Sustainable Resource Science, 1-7-22 Suehiro, Tsurumi, Yokohama,
15 230-0045 Japan

16 *Current address: School of Biological and Biomedical Sciences, Durham University,
17 Durham, DH1 3LE, UK.

18 Corresponding Author: Siobhan Brady: sbrady@ucdavis.edu

19

20 **Short title:** A multi-tier PRC2 regulatory network

21

22 **One-sentence summary:** Chromatin-modifying PRC2 subunits were shown to regulate
23 root vascular development, and their upstream regulators were identified and shown to
24 control the expression of PRC2 downstream targets.

25

26 The authors responsible for distribution of materials integral to the findings presented in
27 this article in accordance with the policy described in the Instructions for Authors
28 (www.plantcell.org) are: Siobhan M. Brady (sbrady@ucdavis.edu) and Miguel de Lucas
29 (miguel.de-lucas@durham.ac.uk).

30

31

32 **ABSTRACT**

33 Spatiotemporal regulation of transcription is fine-tuned at multiple levels, including
34 chromatin compaction. Polycomb Repressive Complex 2 (PRC2) catalyzes the
35 trimethylation of Histone 3 at lysine 27 (H3K27me3), which is the hallmark of a repressive
36 chromatin state. Multiple PRC2 complexes have been reported in *Arabidopsis thaliana* to
37 control the expression of genes involved in developmental transitions and maintenance of
38 organ identity. Here, we show that PRC2 member genes display complex spatiotemporal
39 gene expression patterns and function in root meristem and vascular cell proliferation and
40 specification. Furthermore, PRC2 gene expression patterns correspond with vascular and
41 non-vascular tissue-specific H3K27me3-marked genes. This tissue-specific repression via
42 H3K27me3 regulates the balance between cell proliferation and differentiation. Using
43 enhanced yeast-one-hybrid analysis, upstream regulators of the PRC2 member genes are
44 identified, and genetic analysis demonstrates that transcriptional regulation of some PRC2
45 genes plays an important role in determining PRC2 spatiotemporal activity within a
46 developing organ.

47

48 INTRODUCTION

49 The formation of new organs involves transcriptional reprogramming of pluripotent stem
50 cells in order to give rise to different cell types. This temporal and spatial regulation of
51 gene expression are regulated at multiple levels, including chromatin compaction via
52 histone post-translational modifications, a general mechanism by which promoter
53 accessibility is regulated to enable interaction with transcription factors and RNA
54 polymerase machinery. Despite the extensive chromatin modification data generated in
55 recent years, few studies have evaluated the transcriptional regulation of chromatin
56 modifiers themselves. Polycomb Repressive Complex 2 (PRC2) catalyzes the
57 trimethylation of Histone 3 protein at the lysine 27 position (H3K27me3), the hallmark of a
58 silent chromatin state that is correlated with gene repression and its maintenance across
59 cell division.

60 PRC2 structure is highly conserved, with four core sub-units conventionally named after
61 their homologs in *Drosophila*, including an Enhancer of zeste (E(z)) catalytic SET domain-
62 containing protein, an Extra sex combs (Esc) protein, a nucleosome remodeling factor
63 WD40-containing protein (Nurf55), and a Suppressor of zeste 12 zinc finger protein in a
64 stoichiometric ratio of 1:1:1:1 (Ciferri et al., 2012). However, the number of genes that
65 encode each sub-unit varies between species (Mozgová and Hennig, 2015). The
66 *Drosophila* genome has been described as containing a single gene for each subunit,
67 which consequently constitute a single complex. However, two copies of the Extra sex
68 combs gene, *ESC* and *ESCL*, have been reported (Ohno et al., 2008). In mouse and
69 human there are two copies of the E(z) gene – *EZH1* and *EZH2* (Ciferri et al., 2012;
70 Margueron et al., 2008). In addition, distinct isoforms of Esc have been reported in human
71 (Mozgová and Hennig, 2015; Kuzmichev et al., 2005). The *Arabidopsis thaliana* genome
72 encodes three homologous genes for the E(z) methyltransferase subunit, *MEDEA (MEA)*,
73 *CURLY LEAF (CLF)* and *SWINGER (SWN)*, one for Esc, *FERTILIZATION*
74 *INDEPENDENT ENDOSPERM (FIE)*, five WD40-containing protein genes, *MULTICOPY*
75 *SUPPRESSOR OF IRA1-5 (MSI1–5)*, and three Su(z)12, *FERTILIZATION INDEPENDENT*
76 *SEED2 (FIS2)*, *EMBRYONIC FLOWER2 (EMF2)* and *VERNALIZATION2 (VRN2)*.
77 Together, these subunits have been reported to form three PRC2 complexes, with the
78 methyltransferases acting partially redundantly (Ohno et al., 2008; Chanvivattana et al.,
79 2004; Bemer and Grossniklaus, 2012). Several thousand genes are regulated by PRC2,
80 and distinct complexes have been reported to regulate the expression of genes involved in
81 developmental transitions (Bouyer et al., 2011; Zhang et al., 2007a). The FIS2 complex

82 comprises FIS2, FIE, MEA, and MSI1 and functions in the female gametophyte and
83 endosperm to repress *PHERES* (Köhler et al., 2005). The expression of key regulators of
84 the vegetative-to-reproductive transition, such as *LEAFY* and *AGAMOUS*, are regulated by
85 the EMF2 complex (EMF2, FIE, CLF or SWN and MSI1) (Kinoshita et al., 2001). A third
86 complex (VRN2), which comprises VRN2, FIE, CLF or SWN and MSI1, represses
87 *FLOWERING LOCUS C* to accelerate flowering in response to cold (De Lucia et al., 2008).

88 The regulatory mechanisms that determine which of these complexes are able to act at
89 these specific developmental transitions are unclear. Here, we describe spatiotemporal
90 transcriptional regulation of PRC2 genes in the Arabidopsis root and characterize their
91 function in cellular patterning, proliferation and differentiation. The Arabidopsis root has a
92 simple structural and functional organization consisting of concentric cylinders of cell
93 layers with radial symmetry. Briefly, root growth and development rely on the continuous
94 activity of the apical meristem, where multipotent stem cells surround a small population of
95 centrally located organizing cells, the quiescent center (Scheres, 2007; Terpstra and
96 Heidstra, 2009). Owing to a stereotypical division pattern, stem cells, depending on their
97 position, give rise to different cell files in which the spatial relationship of cells in a file
98 reflects their age and differentiation status (Benfey and scheres, 2000; Dolan et al., 1993).
99 The epidermis is present on the outside and surrounds the cortex, endodermis and
100 pericycle layers. The internal vascular cylinder consists of xylem, phloem and procambium
101 tissues.

102 Here we demonstrate that PRC2 controls root meristem development and regulates
103 vascular cell proliferation in the maturation zone. Distinct suites of genes are marked by
104 H3K27me3 in vascular and non-vascular cells to regulate the balance between cellular
105 proliferation and differentiation. Dozens of transcription factors bind to the promoters of
106 genes that encode PRC2 subunits and regulate their expression in Arabidopsis. Together,
107 this multilayered regulatory network provides key insights into the varied means by which
108 gene expression is regulated to ensure appropriate morphogenesis and functioning of a
109 plant organ.

110 **RESULTS**

111 **PRC2 subunits show regulated transcript and protein abundance in the Arabidopsis** 112 **root**

113 A variety of PRC2 complexes act at distinct developmental transitions during the
114 Arabidopsis life cycle (Kinoshita et al., 2001; Chanvivattana et al., 2004). Spatial and

115 temporal gene expression data in the Arabidopsis root (Supplemental Figure 1) suggest
116 that transcriptional regulation may be an important component in determining the presence
117 of specific PRC2 genes in different cell types. SWN, EMF2 and VRN2 proteins have
118 previously been reported in the root meristem and in root hairs (Ikeuchi et al., 2015). To
119 further validate the spatiotemporal expression pattern of PRC2 subunits, we generated
120 transcriptional fusions for each PRC2 gene (Figure 1A-H) and studied the respective
121 reporter expression pattern within the root. *MEA* was not expressed within the root, while
122 *FIS2* was expressed in the columella (Figure 1C,F). The potential promoter regions of
123 most subunits drove strong expression in all cell types in the meristematic zone that then
124 became preferentially detectable in the vascular cylinder in the elongation and maturation
125 zones (Figure 1A-H). *CLF* in particular showed enrichment in the root vasculature in both
126 the meristem and maturation region of the root, and this was corroborated by an *in situ*
127 hybridization with a probe to the *CLF* transcript (Figure 1E, Supplemental Figure 2D).
128 Translational fusions, for all but *FIS2*, were then used to determine if further regulatory
129 mechanisms might also affect PRC2 protein abundance. SWN protein abundance was
130 enriched within the epidermal and ground tissue layers in the meristem (Figure 2C). The
131 CLF protein, in a complemented *clf-29* mutant background, was found in the root meristem
132 and enriched in the vascular tissue in the maturation zone (Figure 2E, Supplemental
133 Figure 3B). CLF protein in a complemented *clf-28swn-7* background shows the same
134 enrichment patterns (Supplemental Figure 2E). Within the root meristem and elongation
135 zone, SWN, EMF2, VRN2 and FIE (in a complemented *fie-1* mutant background) proteins
136 are present (Figure 2A, B, C, F) (Ikeuchi et al., 2015; Kinoshita et al., 2001). In the
137 differentiation zone, however, SWN, EMF2, VRN2 and FIE proteins are present primarily
138 in vasculature (Figure 2A, B, C, F), although VRN2, EMF2 and SWN protein has also been
139 reported in root hairs (Ikeuchi et al., 2015).

140 **PRC2 activity is required for proper root development**

141 The expression and protein abundance patterns of PRC2 genes suggested that PRC2
142 might influence cell patterning or specification in the Arabidopsis root. Since the *MEA*
143 protein is not found within the Arabidopsis root, *CLF* and *SWN* are the only
144 methyltransferases that are candidate regulators of root development. To test the
145 consequences of loss of PRC2 in root cell specification and patterning, we analyzed the
146 phenotypes of *clf-28 swn-7*, which produce viable embryos with PRC2 function eliminated
147 after germination. In agreement with (Lafos et al., 2011), the *clf-28 swn-7* mutants showed
148 a complete loss of H3K27me3 deposition, as revealed using whole mount

149 immunocytochemistry (Figure 3A,B). However, both the *clf-29* and *swn-7* single mutants
150 show nuclear H3K27me3 (Supplemental Figure 3, 4), suggesting that these proteins have
151 partially redundant functions. Analysis of the single and double mutant combinations of
152 CLF and SWN demonstrated that they interact genetically. The *swn-7* allele has a shorter
153 root with no difference in meristem size, while *clf-29* shows no difference in root length but
154 has a significant increase in the number of cells in the root meristem, as previously
155 reported (Figure 3J-K) (Aichinger et al., 2011). The roots of *clf-28 swn-7* double mutants
156 are shorter than those of wild type, with a small meristem containing fewer cells (Figure
157 3C-D,J-K), as does a *clf-29 swn-7* double mutant (Supplemental Figure 5C-D). Although
158 no defects in radial cell patterning were observed, the number of cells in the vascular
159 cylinder was significantly increased (Figure 3E-G,I Supplemental Figure 5A). In striking
160 similarity with the *clf-28 swn-7* phenotype, the *fie* mutant (Bouyer et al., 2011) displayed a
161 smaller meristem with fewer cells (Supplemental Figure 5B) in addition to a large increase
162 in the number of cells within the vascular cylinder (Figure 3G). This increase in vascular
163 cell number was characterized by an increase in protoxylem and metaxylem cells (Figure
164 3L-M).

165 Although there are several MSI1 homologs, immunopurification experiments determined
166 that MSI1 is the primary WD40 protein required for PRC2 activity in Arabidopsis
167 (Derkacheva et al., 2013). It should be noted however, that MSI1 is also a member of
168 other chromatin modifying complexes (Jullien et al., 2008). Given the vascular phenotypes
169 of mutations in other PRC2 genes and in order to circumvent the female gametophytic
170 lethality of *msi1* mutants (Köhler et al., 2003), we generated a transgenic line that
171 expressed an artificial miRNA (amiRNA) targeting *MSI1* under the *WOODEN LEG (WOL)*
172 promoter (*WOL_{pro}:amiRNA_MSI1*) (Inoue et al., 2001), the expression of which is
173 restricted to the vascular cylinder of the root. To validate *MSI1* silencing, we introduced the
174 transgene into a line containing *MSI1_{pro}:MSI1:GFP* (Figure 3N,O). We tested for changes
175 in H3K27me3 deposition in *MSI1* silenced lines and observed a reduction specifically in
176 the vascular cylinder (Supplemental Figure 6). The *MSI1_{pro}:MSI1:GFP* signal was
177 undetectable in the *WOL_{pro}:amiRNA_MSI1* vascular cylinder (Figure 3I-J). Silencing of
178 *MSI1* in the vascular cylinder was sufficient to decrease overall root growth (Figure 3P,Q),
179 with fewer cells in the meristem, similar to the phenotypes observed in *clf-28 swn-7* and *fie*.
180 However, in contrast to *clf-28 swn-7* and *fie*, which showed an increase in cell number, a
181 statistically significant decrease in vascular cell number was observed (Figure 3G,M).

182 Taken together, our results indicate that PRC2 regulates both root meristem cell number
183 and vascular cell proliferation.

184 **Genes specifically marked by H3K27me3 in vascular and non-vascular tissue**

185 Many genes marked by H3K27me3 have distinct cell type or tissue-specific expression
186 patterns (Turck et al., 2007; Zhang et al., 2007a; Deal and Henikoff, 2010; Lafos et al.,
187 2011) and the data presented above suggested that PRC2 likely regulates the expression
188 of many genes in the vasculature as well as in other cell types within the root. In order to
189 identify the genes specifically marked by H3K27me3 in the vascular tissue relative to the
190 whole root, we carried out fluorescent activated cell sorting using the WOL_{pro}:GFP marker
191 line (Birnbaum et al., 2003) (Supplemental Figure 7A-C) coupled with ChIP-seq using an
192 antibody specific for H3K27me3. As a control, we also carried out ChIP-seq with an
193 antibody specific for H3K4me3, a chromatin modification associated with expressed genes.
194 As expected from previous reports (Zhang et al., 2007b; Roudier et al., 2011), genes
195 marked with H3K27me3 showed lower expression relative to genes with H3K4me3 (Figure
196 4A). Comparison between the list of genes marked by H3K27me3 in the WOL_{pro}
197 population and in the root protoplast population (Figure 4B) identified 130 genomic regions
198 marked by H3K27me3 specifically in the vascular cylinder (Figure 4B). In comparison,
199 2859 genes were specifically enriched in H3K27me3 outside of the vascular tissue
200 (Supplemental Data Set 1). To identify biological processes over-represented in
201 H3K27me3-marked regions associated with the WOL_{pro}:GFP sorted population relative to
202 the whole root population, we carried out Gene Ontology (GO) enrichment analysis (Du et
203 al., 2010). Among these lists of H3K27me3-marked genes, 113 and 82 GO categories
204 were significantly enriched in the WOL_{pro}:GFP population and the whole root population,
205 respectively (Supplemental Data Set 1). 37 GO terms were enriched only in the
206 WOL_{pro}:GFP population, while 6 GO terms were enriched only in the whole root
207 population and thus may represent non-vascular-specific GO terms, although they were
208 not significantly under-represented within the WOL_{pro}:GFP population (Supplemental
209 Figure 6D, Supplemental Data Set 1). The set of non-vascular-specific GO terms are
210 consistent with repression of biological processes associated with vascular development
211 and include axis specification, adaxial/abaxial pattern formation, meristem maintenance,
212 phloem or xylem histogenesis, xylem development, and cell wall organization or
213 biogenesis. In the WOL_{pro}:GFP -specific samples, H3K27me3-marked genes were
214 enriched for floral development, gibberellin-related processes and terpenoid metabolism,
215 suggesting differential regulation of these pathways within vascular cells.

216 **Functional importance of tissue-specific PRC2-mediated repression**

217 In order to identify H3K27me₃-marked genes that are transcriptionally repressed in the
218 vascular cylinder or in non-vascular cells, we further restricted the lists of H3K27me₃-
219 marked genes using cell type-specific gene expression data (Brady et al., 2007). The
220 auxin response factor *ARF17* is marked specifically by H3K27me₃ in vascular tissue and
221 is not expressed in the vascular cylinder. This non-vascular expression pattern was
222 confirmed using a transcriptional fusion in which GFP is expressed under the *ARF17*
223 promoter (Figure 4C) (Ciferri et al., 2012; Okushima, 2005). Conversely, *VND7*, a well-
224 described regulator of vascular development, was marked by H3K27me₃ in non-vascular
225 cells and is specifically expressed in vascular tissue, as confirmed by the use of a
226 promoter:reporter (YFP) fusion (Mozgová and Hennig, 2015; Yamaguchi et al., 2010)
227 (Figure 4E-F).

228 In order to determine the functional importance of PRC2-mediated repression, we sought
229 to over-ride/bypass the silencing in the vasculature presumably conferred by the PRC2 by
230 expressing *ARF17* under the control of a β -estradiol-inducible promoter (Ohno et al., 2008;
231 Coego et al., 2014). This is a similar approach to one described for *AGAMOUS*, a PRC2
232 target gene (Ciferri et al., 2012; Sieburth and Meyerowitz, 1997; Margueron et al., 2008)
233 and other target genes (Mozgová and Hennig, 2015; Ikeuchi et al., 2015; Kuzmichev et al.,
234 2005). The constitutive induction of *ARF17* in the root caused a loss of organization of the
235 root pattern, with frequent observations of ectopic cell proliferation (Figure 4G-J and
236 Supplemental Figure 3A). In contrast, ectopic expression of *VND7* with the β -estradiol-
237 inducible promoter induced ectopic xylem cell differentiation, as has been previously
238 reported (Ohno et al., 2008; Kubo, 2005; Chanvivattana et al., 2004; Bemer and
239 Grossniklaus, 2012) (Figure 4E-F, K-L). Thus, these PRC2-target genes regulate the
240 correct balance between cell proliferation and cell differentiation.

241 **Transcriptional regulation of PRC2 core components in the Arabidopsis root**

242 The differential spatiotemporal expression patterns of PRC2 genes suggest a regulatory
243 role for transcription factors in determining this specificity. We thus utilized the 5' flanking
244 regions upstream of the translational start site of PRC2 genes in the synthesis of the
245 transcriptional fusions as bait in an enhanced yeast one-hybrid assay (Bouyer et al., 2011;
246 Lee et al., 2006; Zhang et al., 2007a; Brady et al., 2011; Taylor-Teeples et al., 2015). In
247 order to focus on the vascular-specific regulation of these genes, we screened the
248 promoters against a set of root vascular-expressed transcription factors (Köhler et al.,

249 2005; Gaudinier et al., 2011) (Kinoshita et al., 2001; Reece-Hoyes et al., 2011)
250 (Supplemental Data Set 2). In total, 101 transcription factors (out of 653) interacted with
251 these potential promoters (Figure 5), with ten TF families over-represented (C2H2, bHLH,
252 Homeobox, MYB, AP2-EREBP, WRKY, GRAS, bZIP, C2C2-Dof, and ARF; p-value < 0.01).
253 In order to validate these transcription factor-promoter interactions *in planta*, we performed
254 two types of assays. Transcription factors were overexpressed using a β -estradiol-
255 inducible system (De Lucia et al., 2008; Coego et al., 2014) and expression of the
256 respective target gene was measured 24 hours after induction (Supplemental Data Set 3).
257 In addition, myc-tagged transcription factors were assessed for their ability to drive
258 expression of the GUS reporter gene fused to the target promoter in *Nicotiana*
259 *benthamiana* leaves (Supplemental Data Set 3). Altogether, 71 of the 101 transcription
260 factors in the network were tested in these *in planta* assays and a total of 63 interactions
261 were successfully validated *in planta* (Supplemental Data Set 3, Figure 5, Supplemental
262 Figure 8). We hypothesize that these transcription factors represent an important upstream
263 regulatory component of PRC2 gene expression. We next postulated that distinct TFs
264 could control the expression of PRC2 genes in different cell types. To address this
265 question, we investigated the co-expression patterns between each TF and their target
266 gene using spatial root transcriptome data (Scheres, 2007; Brady et al., 2007; Terpstra
267 and Heidstra, 2009) (Supplemental Figure 7). A total of 9 TF-promoter interactions were
268 significantly and highly correlated across cell types ($r \geq \pm 0.6$) (Supplemental Data Set 3).
269 Together, our data demonstrate that a diverse set of transcription factors is sufficient to
270 regulate PRC2 expression *in planta*, along with other factors including the regulation of the
271 chromatin environment, which likely act in a combinatorial regulatory code to specify PRC2
272 gene expression.

273 **Transcriptional Regulation of PRC2 Components Contributes to PRC2-Mediated** 274 **Regulation of Cell Proliferation and Differentiation**

275 In order to determine the functional contribution of transcription factors controlling PRC2
276 gene expression that in turn regulate the expression of PRC2 target genes, we focused on
277 the DOF6 transcription factor, which activates *CLF* expression both in transient and
278 estradiol induction assays (Supplemental Data Set 1 and 3). The induction of *DOF6*
279 causes severe inhibition of root growth but increases the number of cells in the meristem
280 (Figure 6A, Supplemental Figure 2A-B). Both *DOF6* and *CLF* are also both expressed in
281 root vascular tissue, further supporting the possibility of this regulatory interaction *in planta*
282 (Rueda-Romero et al., 2012) (Figure 1E and Supplemental Figure 2C-D). Since DOF6 is

283 sufficient to increase *CLF* expression (Figure 6C), our hypothesis was that *DOF6*
284 overexpression could lead to an increase in *CLF* expression in non-vascular tissue, which
285 in turn could result in an increase in PRC2 activity in these cell types, as determined by
286 measuring gene expression and corresponding H3K27me3 levels. Our H3K27me3 ChIP-
287 seq data demonstrate that *ARF17* is a vascular-specific target of PRC2, and the
288 transcriptional fusion data demonstrate that *ARF17* is only expressed outside of the
289 vasculature (Figure 4C, Supplemental Data Set 1). *ARF17* is a target of PRC2 complexes
290 containing CLF but not SWN based on the increase in gene expression in *clf-29* versus
291 *swn-7* mutants (Figure 6B). Furthermore, overexpression of a miRNA160-resistant version
292 of *ARF17* results in prominent vegetative and floral defects similar to those observed in *clf-*
293 *29*, including upward curling of leaf margins, reduced plant size, accelerated flowering time,
294 and reduced fertility (Kinoshita et al., 2001; Mallory, 2005; Chanvivattana et al., 2004). We
295 thus chose *ARF17* as a candidate to explore the influence of PRC2 gene expression
296 manipulation on its target gene (*ARF17*) expression.

297

298 Over-expression of *DOF6* led to increased expression of *CLF* concomitantly with a
299 decrease in *ARF17* expression (Figure 6C). This decrease in *ARF17* expression is
300 dependent on CLF, as shown in the *DOF6* estradiol-inducible line in the *clf-29* mutant
301 background (Figure 6E). Furthermore, the domain of *ARF17* expression expanded to the
302 vascular cylinder in a *clf-29* mutant background (Figure 6F), demonstrating that CLF is
303 sufficient to regulate the spatial expression pattern of *ARF17*. Finally, H3K27me3 of
304 *ARF17* is increased upon *DOF6* induction (Figure 6D), demonstrating that *DOF6* increases
305 the expression of *CLF* and, in turn, CLF regulates the expression of the target gene
306 *ARF17* through changes in H3K27me3. An additional influence of CLF was observed with
307 respect to the regulation of root length. When the *clf-29* mutation was introduced into the
308 *DOF6* estradiol-inducible line, upon estradiol induction, no influence on root length was
309 observed. Thus, we identified transcription factors that are sufficient to control the
310 expression of PRC2 genes in the root, and we demonstrated that altered expression of
311 these transcription factors can disrupt the expression of a PRC2 subunit gene in addition
312 to the levels of H3K27me3 and the corresponding expression of its target gene.

313 **DISCUSSION**

314 **A Multi-tiered Regulatory Network for Gene Expression**

315 We systematically characterized the regulation of PRC2 gene expression at cell type-
316 resolution using Arabidopsis roots as a model system. We showed that there are distinct
317 spatial and temporal transcript accumulation patterns for PRC2 components. The
318 heterologous (yeast/*N. benthamiana*) and *in vivo* (Arabidopsis) approaches we employed
319 revealed a transcriptional network that controls PRC2 gene expression in the Arabidopsis
320 root. Altogether, our data provide evidence that transcriptional control of the PRC2
321 component *CLF*, and likely of other PRC2 components, plays an important role in
322 determining H3K27me3 levels and the corresponding expression of H3K27me3 targets in
323 a spatiotemporal manner. This regulation is likely complemented by other previously
324 described modes of regulation in Arabidopsis, including *cis*-regulatory regions similar to
325 the Polycomb Repressive Element in *Drosophila* (Ikeuchi et al., 2015; Deng et al., 2013),
326 long non-coding RNAs, and protein–protein interactions via Polycomb Repressive
327 Complex 1 (PRC1) and PRC1-like genes to determine target specificity and chromatin
328 compaction (Ikeuchi et al., 2015; Margueron and Reinberg, 2011).

329 Further dissection of these distinct tiers of this regulatory network is needed. At the upper
330 level of the network, the correlation of expression between transcription factors and their
331 target PRC2 genes (Gu et al., 2014; Brady et al., 2007) suggests that distinct groups of
332 transcription factors regulate the expression of these genes in space, in time, or in both
333 space and time (Supplemental Data Set 1). At the second tier of the network, analyses of
334 PRC2 gene mutants demonstrated that *CLF*, *SWN* and *FIE*, key components of PRC2,
335 functionally regulate root meristem and vascular development, likely at the level of cell
336 division. Additionally, the translational fusion patterns suggest that only a restricted
337 number of complexes can form at a particular cell type or temporal stage of development.
338 It will be interesting in the future to determine if the cell type- or tissue-specific expression
339 patterns of *CLF* or *SWN* are necessary to regulate the H3K27me3 of distinct suites of
340 genes. In addition, in proximal meristematic vascular tissue, *CLF* and *SWN* protein were
341 both present. The mechanism by which different complexes form and how the affinity for
342 different targets is determined remain to be described. At the final tier of the network,
343 whether distinct PRC2 complexes regulate distinct groups of genes within the root
344 meristem remains to be determined. However, our data showing vascular-specific
345 H3K27me3 and silenced genes provide proof of such suites of genes at the level of
346 individual tissues.

347 **Regulation of Cell Proliferation and Differentiation during Arabidopsis Root**
348 **Development**

349 In plants, PRC2 proteins maintain organ and cell-type identity, regulate developmental
350 transitions, repress cell proliferation (Lafos et al., 2011; Hennig and Derkacheva, 2009)
351 and regulate totipotency (Aichinger et al., 2009; He et al., 2012). Here, we report two
352 additional functions of PRC2 in post-embryonic development: the regulation of cell
353 proliferation in vascular tissue, and the appropriate execution of xylem cell differentiation
354 (Figure 3E-G; L-M). In the developing root, procambium cells are the stem cell source
355 responsible for vascular cell types and secondary growth (Bouyer et al., 2011; Mahonen,
356 2006; 2000; De Rybel et al., 2014). Procambium cells proliferate and can undergo
357 differentiation into either xylem cells or phloem cells depending on positional cues
358 (Derkacheva et al., 2013; Fisher and Turner, 2007; Etchells et al., 2013; Etchells and
359 Turner, 2010). The vascular proliferation phenotype of the *clf-28 swn-7* mutant suggests
360 that PRC2 represses division of the procambium cell population. *CLF* and *SWN* are not
361 responsible for initiating division of these cells, but rather, when the appropriate number of
362 cells has been produced, PRC2 activity likely negatively influences chromatin accessibility
363 for transcription factors such as *ARF17* in addition to cell cycle regulators. The over-
364 proliferation phenotype of the *ARF17* over-expressor and its similarity to the phenotype of
365 the *clf28swn7* mutant suggest that *ARF17* may be such a cell cycle regulator. The lack of
366 a vascular phenotype in the *clf29* mutant implies that cell proliferation is likely also
367 controlled by other *SWN*-dependent H3K27me3 targets. On the other hand, the *fie-042*
368 ectopic xylem cell phenotype, the tissue-specific *VND7* H3K27me3 deposition pattern, and
369 the finding that over-riding this repression through ectopic expression results in ectopic
370 xylem differentiation suggest that tissue-specific PRC2 activity ensures the appropriate
371 execution of the xylem cell differentiation program.

372

373 Knockdown of *MSI1* in the vascular tissue resulted in a very different phenotype relative to
374 that observed in mutants of other PRC2 subunits. In the vascular cylinder, the planes of
375 division were altered suggesting that this particular gene likely plays a role in procambium
376 cell patterning. Interestingly, *WOL_{pro}:amiRNA_MSI1* expression resulted in a short root
377 phenotype despite being only driven in the vascular cylinder. This could be due to cell
378 non-autonomous effects, defects in vascular development influencing overall growth, or a
379 defect in the vascular initial cells, which determine quiescent cell identity. *MSI1* is a
380 member of other chromatin modifying complexes including the CAF1 complex, which is
381 associated with nucleosome deposition for chromatin assembly and histone deacetylation
382 (Jullien et al., 2008; Hennig et al., 2003). Thus, the phenotypes observed may reflect

383 developmental decisions occurring during early root patterning or independent of PRC2
384 activity.

385 **A Comparative Perspective on PRC2 Function in Plants and Animals**

386 In animal embryonic stem cells and outside of the embryo, PRC2 is required for the
387 maintenance of differentiation potential (Köhler et al., 2003; Laugesen and Helin, 2014).
388 Mutations in PRC2 subunits can either delay differentiation of myogenic or neurogenic cell
389 types or precociously advance the differentiation of particular cell types in addition to
390 preserving the appropriate cell identity (Inoue et al., 2001; Stojic et al., 2011; Pasini et al.,
391 2007; Hirabayashi et al., 2009; Fasano et al., 2007; Sher et al., 2008; Aldiri and Vetter,
392 2009). In contrast, in the plant procambial stem cell population, PRC2 regulates self-
393 renewal capabilities (Turck et al., 2007; Laugesen and Helin, 2014; Zhang et al., 2007a;
394 Deal and Henikoff, 2010; Lafos et al., 2011). Our data also demonstrate that in root cells,
395 PRC2 ensures the correct cell type-specific differentiation state through spatially
396 repressing the expression of cell type-specific developmental regulators (VND7). Thus, in
397 plants, PRC2 regulates self-renewal of the procambial stem cell population in addition to
398 cell differentiation-

399 Uncontrolled abundance, increased activity, or loss of function of PRC2 components can
400 lead to disease (Birnbaum et al., 2003; Bracken et al., 2003; Kleer et al., 2003; Takawa et
401 al., 2011; Varambally et al., 2002; Wagener et al., 2010). Thus, our findings indicate that
402 transcription factors may be an important component in determining PRC2 gene
403 expression in animals, and through this mechanism, the repression of their targets.
404 Furthermore, in cases where multiple genes have been found to encode a single PRC2
405 subunit, the expression patterns of these subunits and their upstream regulation should be
406 systematically explored. Epigenetic abnormalities are common in human cancer and play
407 a key role in tumor progression, and hence, significant efforts have focused on developing
408 inhibitors of these PRC2 proteins to treat disease (Zhang et al., 2007b; Helin and Dhanak,
409 2013; Roudier et al., 2011). The characterization of cell type or tissue-specific regulation of
410 PRC2 gene expression may provide an additional mode by which the negative effects
411 caused by PRC2 misregulation could be abrogated.

412 **METHODS**

413 **Plant material**

414 All transgenic *Arabidopsis thaliana* plants and mutants are in the Col-0 background except
415 for the VRN2_{pro}:VRN2:GUS line (kindly provided by Caroline Dean), which is in the Ler

416 background, as is the FIEpro:FIE:GFP line (Kinoshita et al., 2001). The *clf-28 swn-7*
417 (SALK_139371, SALK_109121), *clf-29* (SALK_021003), *swn-7* (SALK_109121), and *fie*
418 (SALK_042962) (Du et al., 2010; Bouyer et al., 2011) mutants were kindly provided by
419 François Roudier and Daniel Bouyer, respectively. The DOF6 β -estradiol inducible, VND7
420 and ARF17 transcriptional and FIE in *fie-1*, SWN and MEA in *mea-3* translational fusions
421 have been described elsewhere (Brady et al., 2007; Rueda-Romero et al., 2012;
422 Yamaguchi et al., 2010; Rademacher et al., 2011) (Yadegari et al., 2000; Wang et al.,
423 2006). Transcription factor-inducible lines were obtained from the TRANSPLANTA
424 collection (Coego et al., 2014).

425 Plants were grown under standard conditions at 24°C in a 16-h light 8-h dark cycle. For
426 root analyses, plants surfaced sterilized and sown in 1% Sucrose Murashige and Skoog
427 (1% MS) medium. Seeds were stratified for 3 days at 4°C and dark and then transferred
428 and kept vertical into a Percival growth chamber with a light intensity of $\sim 700 \text{ mol}\cdot\text{m}^{-2} \text{ s}^{-1}$
429 illuminated by a daylight-white fluorescence lamp (FL40SS ENW/37; PANASONIC).
430 Selection of transgenic seedlings were performed in 1% MS medium supplemented with
431 50 mg L⁻¹ kanamycin or 15 mg L⁻¹ Glufosinate ammonium, depending on the transgene.

432 **Cloning strategies**

433 All oligonucleotides used in this study are described in Supplemental Data Set 4. All PCR-
434 amplified fragments were completely sequenced after subcloning, and only the clones
435 without PCR-induced errors were used for subsequent cloning steps. For promoter
436 amplification, Col-0 genomic DNA was used as template. For coding region amplification,
437 Col-0 cDNA was used as template, except for the *CLF* coding region, which was amplified
438 from genomic DNA and thus contains introns. For the generation of the transcriptional
439 GUS fusions, each respective PCR product was introduced into pENTR D-TOPO
440 (Invitrogen) and subsequently recombined into the pGWB4 and pGWB5 destination
441 vectors (Nakagawa et al., 2007) with the exception of the *CLF* promoter, which was
442 assembled to Venus-N7 (rapidly folding YFP variant) by Hot Fusion reaction (Fu et al.,
443 2014) into the Bsal digested pGoldenGate-Se7 (Shahram Emami, 2013).

444

445 For the CLF translational fusion shown in Figure 2, the *CLF* genomic region was amplified
446 (primers CLF_TOPO_F_NO_ATG/CLF_R) and introduced into pENTR™/D-Topo®
447 (Invitrogen). The gCLF_D_Topo clone was introduced into the pB7WGC2 binary vector to
448 generate a CFP:gCLF fusion. The ECFP:gCLF sequence was then amplified
449 (ECFP_TOPO_F/CLF_R) and introduced into pENTR™/D-Topo®. The -2842 DNA

450 sequence corresponding to the *CLF* promoter was amplified (pCLF_F/pCLF_R) and
451 cloned into pENTR 5'TA-TOPO[®]. A MultiSite Gateway reaction was performed using
452 CLFpro-TA-Topo, CFP:gCLF-D-Topo and the pK7m34GW destination vector. The
453 CLFpro:CFP:gCLF transgene was introduced into the *clf-29* background by floral dip
454 transformation {Clough:1998uf}, and a complementation assay was performed on T2
455 plants to validate a 3:1 segregation ratio. For the *CLF* genomic fusion shown in
456 Supplemental Figure 7B, a genomic region of *CLF* including 2175 bp upstream from the
457 start codon and 1010 bp downstream from the stop codon was amplified with primers D-
458 TOPO-genomic_CLF_s2 and genomic_CLF_as2, following with primers genomic_CLF_s1
459 and genomic_CLF_as1, using PrimeSTAR[®] Max DNA polymerase (Takara). The PCR
460 product was cloned into pENTR[™]/D-Topo[®] (Thermo Fisher scientific), and an error-free
461 entry clone, pENTR-gCLF, was confirmed by sequence analyses. A mGFP sequence with
462 a GGS-linker at its N-terminus was inserted into pENTR-gCLF at the site before the stop
463 codon of CLF in frame by CPEC (circular polymerase extension cloning) method, following
464 the amplification of pENTR-gCLF and linker-mGFP with primers CLF ter_s and CLF body-
465 Δstop_as and primers CLF body-mGFP_s and mGFP-CLF ter_as, respectively. A
466 recombination reaction was performed between the resulting entry clone, pENTR-gCLF-
467 mGFP, and destination vector pGWB501 (Nakagawa et al., 2007) using LR Clonase II
468 enzyme mix (Invitrogen[™]). Error-free destination clone was confirmed by sequence
469 analyses and introduced into *Agrobacterium tumefaciens* strain GV3101::pMP90 by
470 electroporation. The transgene was introduced into the *clf-28+/-; swn-7-/-* background by
471 floral dip transformation of *clf-28+/-; swn-7-/-* plants. A complementation assay was
472 performed to validate the function of the fusion protein. For the other translational GFP
473 fusions, gene promoters were also introduced into pENTR 5'TA-TOPO[®]; gene cDNAs
474 were introduced into pENTR D-TOPO, and the *mGFP5* reporter gene was introduced into
475 pDONOR P2r-P3. Plasmids containing the promoter, gene and *GFP* were introduced into
476 pB7m34GW (Karimi et al., 2005) by a Multisite Gateway reaction (Invitrogen).

477

478 The design of the artificial miRNA for *MSI1* was performed following WMD3 software
479 (Ossowski et al., 2008) and cloned into pENTR D-TOPO. Afterwards, a Multisite Gateway
480 reaction was performed in combination with the promoter of *WOODEN LEG* (kindly
481 provided by Anthony Bishopp -University of Nottingham) and pK7m24GW (Karimi et al.,
482 2005). The resulting plasmids were introduced into *Agrobacterium tumefaciens* strain
483 GV3101 carrying the pSoup plasmid (Hellens et al., 2000), and Col-0 wild type in addition

484 to MSI1_{pro}:MSI1:GFP were transformed using floral dip (Clough and Bent, 1998).
485 Transformation into the MSI1_{pro}:MSI1:GFP background served as a control to ensure
486 precise tissue-specific silencing of MSI1 with the designed artificial miRNA.

487 **Arabidopsis cross-sections**

488 Five-day-old roots were embedded in 3% agarose (PELCO® 21 Cavity EM Embedding
489 Mold) and incubated overnight at 4°C in Fixation Buffer (2.5% glutaldehyde + 2%
490 paraformaldehyde in phosphate buffer 0.2M (pH 7). Dehydration was performed by
491 incubating the sample for 2h in serial dilutions of ethanol (20%, 40%, 60%, 80%, 90% and
492 95%). The sample was plastic embedded by performing the following steps: 2 hours
493 incubation in 1:1 Ethanol:Acetone, 2 hours incubation in 100% Acetone, 12 hours
494 incubation in 7:1 Acetone:Spurr's resin, 12 hours incubation in 3:1 Acetone:Spurr's resin,
495 12 hours incubation in 100% Spurr's resin, 12 hours incubation in Spurr's resin. The resin
496 was polymerized at 70°C for 12 hours. Blocks were trimmed and 1.5 µM cross-sections
497 were produced with a Leica 2050 SuperCut microtome. Toluidine blue staining (0.1% of
498 Toluidine blue in 0.1M Phosphate buffer pH 6.8) was performed before microscopic
499 analysis.

500

501 The mPS-PI staining method (Truernit et al., 2008) combined with confocal microscopy
502 was used for the acquisition of high resolution root longitudinal and Z-stack images of
503 ARF17ox plants under Mock and β-Estradiol treatments.

504 **Gene regulatory network mapping**

505 Promoter sequences for PRC2 genes are described in Supplemental Data Set 2. Yeast
506 One Hybrid Screening was performed as described (Gaudinier et al., 2011). Correlations
507 between predicted transcription factors and targets were determined using root spatial
508 temporal microarray datasets found in Brady et al. 2007. For simplicity, the data were
509 transformed to contain the Log(2) mean expression value for each sample. A Pearson
510 correlation was calculated for each network-predicted TF-promoter interaction set.
511 Interactions with a Benjamini-Hochberg FDR corrected p-value less than or equal to 0.05
512 were considered significant. P-values for the Benjamini-Hochberg correction were
513 determined from correlations of all possible TF-promoter combinations of each node within
514 the network.

515

516 Validation and the direction of the yeast one hybrid interactions were characterized *in vivo*
517 by performing *trans*-activation assays in *Nicotiana benthamiana* leaves and gene
518 expression analyses in Arabidopsis estradiol-inducible transcription factor lines. For *trans*-
519 activation assays transcription factors in PYL436 (effector) (Ma et al., 2013), collection
520 kindly provided by Dinesh Kumar – UC Davis, promoter:GUS (reporter),
521 35S_{pro}:LUCIFERASE (internal control) and p19 (RNA silencing inhibitor) constructs were
522 transformed into Agrobacterium tumefaciens (strain GV3101) and used as described in
523 (Taylor-Teeple et al., 2015). In Arabidopsis, 12 hour and 24 hour treatments in liquid 1%
524 MS supplemented with 10 μ M β -Estradiol (from a 10mM stock in 100% DMSO) was used
525 to induce the expression of each transcription factor in 5-day-old seedlings. Quantification
526 of transcription factor and PRC2 gene expression was performed by Reverse-transcription
527 -quantitative PCR. We calculated the mean from 3 independent experiments (biological
528 replicates) and from the average of 3 technical replicates per biological replicate. Each
529 biological replicate captures expression from approximately 200 roots of each respective
530 genotype. In each case, the $\Delta\Delta$ Ct was calculated relative to a Ubiquitin10 control
531 (At4g05320). In all cases, significance was tested using a t-test. * = p<.05; ** = p<.01; ***
532 = p<.001.

533 We used Cytoscape software (Shannon et al., 2003) for data visualization and GO
534 analysis of the network.

535 **Whole mount H3K27me3 immunohybridization of Arabidopsis roots**

536 The protocol was adapted from (She et al., 2014). Roots of 5-day-old plants were fixed in
537 fixation buffer (1xPBS, 2mM EGTA, 1% Formaldehyde, 10% DMSO and 1% Tween-20) for
538 30 minutes at room temperature and then mounted in 5% Acrylamide on a microscope
539 slide. Samples were fixed by incubating them for 5 minutes in 100% ethanol, 5 minutes in
540 100% methanol, 30 minutes in methanol:xylene (1:1), 5 minutes in methanol, 5 minutes in
541 ethanol and 15 minutes in methanol:PBS (1.37M NaCl, 27mM KCl, 100mM Na₂HPO₄,
542 18mM KH₂PO₄, pH 7.4) + 0.1% Tween 20 (1:1) + 2.5% Formaldehyde. The samples were
543 then rinsed with PBS + 0.1% Tween 20 and cell walls were digested for 2h at 37°C with
544 cell wall digestion solution (0.5% cellulase, 1% driselase, 0.5% pectolyase in PBS). After
545 rinsing with PBS + 0.1% Tween 20, the samples were permeabilized in PBS + 2% Tween
546 20 for 2 hours. Immunodetection was performed using antibodies against H3K27me3
547 (Millipore 07-449), H3K4me3 (Millipore 07-473) and H3 (ab1791) as a control at 0.01 μ g/ μ l
548 final concentration each, for 14 hours. Samples were washed for 4hours with PBS + 0.1%

549 Tween 20 and incubated for 12h with goat anti-rabbit (alexa fluor 488 conjugate)
550 secondary antibody (Life Technologies A-11034A). Samples were washed with 1x PBS +
551 0.1% Tween-20 for 1 hour and nuclei were counterstained with propidium iodide at a
552 concentration of 5 µg/ml for 15 min, rinsed with PBS + 0.1% Tween 20, and mounted in
553 Prolong Gold (Invitrogen) + 5 µg/ml propidium iodide. Samples were imaged using a Zeiss
554 700 (Genome Center – University of California, Davis). Simultaneous detection of Alexa
555 fluor 488 and Propidium Iodide signal was performed using the same settings among the
556 different samples/mutants (10-15 roots were studied for each mutant line).

557 **Fluorescence Activated Cell Sorting**

558 Arabidopsis WOL_{pro}:GFP root protoplast were prepared as described in (Brady et al.,
559 2007). The MoFlo cell sorter's electronic configuration was modified to identify intact
560 protoplasts above electronic and sample buffer "noise" levels by choosing a side scatter
561 electronic threshold and by applying logarithmic scaling to the forward angle and side
562 angle 488nm laser light scatter signals. To collect the GFP-positive protoplasts, the green
563 fluorescence of the GFP (530/50 detection filter) was separated from the red fluorescence
564 (emission 670/30) of chlorophyll (Supplemental Figure 5). Protoplast chromatin was
565 crosslinked with 0.1% formaldehyde for 5 min and the reaction was stopped by adding
566 glycine (0.125M final concentration).

567 **Chromatin Immunoprecipitation assay**

568 The chromatin immunoprecipitation assay performed in this study is a modification of the
569 protocol described in (Bouyer et al., 2011). We used four independent biological replicates
570 (100,000 GFP positive protoplast each) and two antibodies: H3K27me3 (Millipore 07-449)
571 and H3K4me3 (Millipore 07-473). DNA recovered after ChIP and the input chromatin were
572 both amplified using a SeqPlex Enhanced DNA amplification kit (SEQXE – Sigma)
573 following the manufacturer's instructions. Amplified DNA was used to synthesize a
574 barcoded Illumina-compatible library (Kumar et al., 2012). Libraries were pooled and
575 sequenced on the HiSeq2000 in the 50SR mode.

576 **ChIPseq data analysis**

577 Reads were filtered by length and quality and aligned to the Arabidopsis (TAIR10) genome
578 using Bowtie (Langmead et al., 2009) and the parameters "-v2 -m1 --best --strata -S".
579 SCICER software was used to determine the differentially methylated islands using a
580 200bp window size, 200bp gap size and an FDR of 0.005. The genomic regions containing
581 the histone modification was determined using windowbed software (Quinlan and Hall,

582 2010) and -1000bp upstream and downstream of the gene body for H3K27me3 and 200bp
583 upstream and 200bp downstream for H3K4me3. Genes that overlap in at least 3 of the 4
584 biological replicates were considered as high confidence genes for the downstream
585 analyses.

586

587 Root cell type-specific expression of the H3K27me3 and H3K4me3 affected genes was
588 obtained from (Brady et al., 2007). Raw expression values were \log_2 transformed and
589 graphed with R software and the ggplot2 package.

590 **GUS expression analysis in Arabidopsis**

591 Plant tissue was fixed in 90% acetone for 30 minutes and washed twice with water before
592 GUS staining. Roots were submerged in the GUS staining solution (50mM Phosphate
593 buffer, 0.2% Triton TX-100, 1.5mM Potassium Ferrocyanide, 1.5mM Potassium
594 Ferricyanide and 2mM X-Gluc (5-bromo-4-chloro-3-indolyl β -D-glucuronide cyclohexamine
595 salt dissolved in DMSO – Gold Biotechnology G1281C1), infiltrated under vacuum for 5
596 minutes, and incubated at 37°C in the dark for 18 hours. Roots were then washed with
597 increasing concentrations of diluted ethanol (20%, 35%, 50% and 70%) and then mounted
598 with Hoyer's solution on microscope slides. The activity of the GUS reporter gene was
599 observed under a Zeiss Axioscope 2 Fluorescence microscope.

600 ***In situ* hybridization**

601 The ARF17 and CLF coding region was PCR amplified using Col0 cDNA and the set of
602 primers "ARF17_cDNA_F"/"ARF17_cDNA_R" and "CLF_TOPO_F_NO_ATG"/
603 CLF_R(no_STOP)". PCR product was cloned into pGEMTeasy (PROMEGA). Fluorescein
604 labeled sense and antisense probes were performed as manufacturer indications
605 (Fluorescein RNA Labeling Mix - Roche). Tissue fixation, permeabilization, probe
606 hybridization and detection were adapted from (Bruno et al., 2011). Probe detection was
607 performed using HRP conjugated anti-FITC antibody (1:100 dilution) (AB6656, Abcam),
608 followed by tyramide signal amplification (TSA™ Reagent, Alexa Fluor® 488 Tyramide –
609 Molecular probes (T20948)). Tissue was then counter stained with propidium iodide
610 (5ug/mL) for 5 min, rinsed in water, and the samples were mounted with antifade reagent
611 (Prolong gold – Molecular probes –(P36941)). Samples were imaged using a Zeiss 880
612 with Ayriscan (SBBS –Durham University). Simultaneous detection of Alexa fluor 488 and
613 Propidium Iodide signal was performed using the same settings among the different
614 samples (10-15 roots were studied for each mutant line).

615

616 **Accession numbers**

617 Sequence data from this article can be found in the GenBank/EMBL libraries under
618 accession numbers GSE86429. Accession numbers of major genes mentioned are as
619 follows: CLF = At2g23380; SWN = At4g02020; DOF6 = At3g45610; VND7 = At1g71930;
620 FIE = At3g20740; ARF17 = At1g77850; MEA = At1g02580; MSI1 = At5g58230; FIS2 =
621 At2g35670; EMF2 = At5g51230; VRN2 = At4g16845.

622

623 **Supplemental Data**

624 **Supplemental Figure 1.**

625 Transcriptional profile of PRC2 genes in the Arabidopsis root.

626 **Supplemental Figure 2.** DOF6 OX root phenotype, DOF6 and CLF root expression and
627 CLF protein abundance in the *clf28swn7* background.

628 **Supplemental Figure 3.** ARF17ox ectopic cell proliferation data, CLFpro:CFP:CLF
629 complementation assay and ARF17 RNA in-situ sense control.

630 **Supplemental Figure 4.** Whole-mount immunostaining of H3K27me3 and H3K4me3
631 deposition in Arabidopsis PRC2 mutant roots.

632 **Supplemental Figure 5.** Root cellular resolution phenotypes of different PRC2 mutants

633 **Supplemental Figure 6.** Whole-mount immunostaining of H3K27me3 in the
634 pWOL:amiRNA_MSI1 Arabidopsis line.

635 **Supplemental Figure 7.** Vascular-specific analysis of H3K27me3 deposition for the
636 fluorescence activated cell sorting of the stele (WOLpro:GFP).

637 **Supplemental Figure 8.** Transcriptional profiles of the transcription factors upstream of
638 PRC2 genes.

639 **Supplemental Data Set 1:** H3K27me3 and H3K4me3 genes in the vascular cylinder and
640 whole root and associated GO categories.

641 **Supplemental Data Set 2:** Protein-DNA Interaction Network and promoter sequences for
642 the different PRC2 genes studied.

643 **Supplemental Data Set 3:** PRC2 Network Validation.

644 **Supplemental Data Set 4:** Primer sequences.

645

646 **ACKNOWLEDGMENTS**

647 MDL was supported by an EMBO and HFSP postdoctoral fellowships. SMB and FR were
648 supported by the France-Berkeley Fund. SMB was supported by a Katherine Esau Junior
649 Faculty Fellowship and a Hellman Fellowship. Work in the Colot's lab was supported by
650 the European Union Seventh Framework Programme Network of Excellence EpiGeneSys
651 and the CNRS (AKM, EC and FR). AKM is the recipient of a grant from the French
652 Ministère de la Recherche et de l'Enseignement Supérieur. Work in the Sugimoto lab was
653 supported by the Grant-in-Aid for Scientific Research on Priority Areas to KS (26291064).
654 This project was supported by the University of California Davis Flow Cytometry Shared
655 Resource Laboratory with funding from the NCI P30 CA0933730, and NIH NCRR C06-
656 RR12088, S10 RR12964 and S10 RR 026825 grants and with technical assistance from
657 Ms. Bridget McLaughlin and Mr. Jonathan Van Dyke. We would like to thank Judy
658 Jernstedt for providing us access to a microtome and to Niko Geldner and Peter Etchells
659 for critical reading of the manuscript.

660

661 **AUTHOR CONTRIBUTIONS**

662 M.D.L. designed and performed experiments, analyzed data, discussed results, and wrote
663 the article. L.P. performed experiments and analyzed data. G.T performed computational
664 analyses. A.G. performed experiments. A.K.M., H.H, D.K, and M.R performed experiments.
665 K.S designed experiments with H.H and analyzed data. F.R. designed experiments with
666 A.K.M, and contributed to writing the manuscript. S.M.B. designed experiments, discussed
667 results, and wrote the article

668

669 **REFERENCES**

670 **Aichinger, E., Villar, C.B.R., Di Mambro, R., Sabatini, S., and Kohler, C.** (2011). The
671 CHD3 Chromatin Remodeler PICKLE and Polycomb Group Proteins Antagonistically
672 Regulate Meristem Activity in the Arabidopsis Root. *The Plant Cell* **23**: 1047–1060.

673 **Aichinger, E., Villar, C.B.R., Farrona, S., Reyes, J.C., Hennig, L., and Köhler, C.**
674 (2009). CHD3 Proteins and Polycomb Group Proteins Antagonistically Determine Cell
675 Identity in Arabidopsis. *PLoS Genet* **5**: e1000605.

676 **Aldiri, I. and Vetter, M.L.** (2009). Characterization of the expression pattern of the PRC2
677 core subunit Suz12 during embryonic development of *Xenopus laevis*. *Dev. Dyn.* **238**:
678 3185–3192.

679 **Bemer, M. and Grossniklaus, U.** (2012). Dynamic regulation of Polycomb group activity

680 during plant development. *Curr. Opin. Plant Biol.* **15**: 523–529.

681 **Benfey, P.N. and scheres, B.** (2000). Root development. *Curr. Biol.* **10**: R813–5.

682 **Birnbaum, K., Shasha, D.E., Wang, J.Y., and Jung, J.W.** (2003). A gene expression
683 map of the Arabidopsis root. *Science*.

684 **Bouyer, D., Roudier, F., Heese, M., Andersen, E.D., Gey, D., Nowack, M.K., Goodrich,
685 J., Renou, J.-P., Grini, P.E., Colot, V., and Schnittger, A.** (2011). Polycomb
686 Repressive Complex 2 Controls the Embryo-to-Seedling Phase Transition. *PLoS
687 Genet* **7**: e1002014.

688 **Bracken, A.P., Pasini, D., Capra, M., Prosperini, E., Colli, E., and Helin, K.** (2003).
689 EZH2 is downstream of the pRB-E2F pathway, essential for proliferation and amplified
690 in cancer. *The EMBO Journal* **22**: 5323–5335.

691 **Brady, S.M. et al.** (2011). A stele-enriched gene regulatory network in the Arabidopsis
692 root. *Molecular Systems Biology* **7**: 459.

693 **Brady, S.M., Orlando, D.A., Lee, J.Y., Wang, J.Y., Koch, J., Dinneny, J.R., Mace, D.,
694 Ohler, U., and Benfey, P.N.** (2007). A High-Resolution Root Spatiotemporal Map
695 Reveals Dominant Expression Patterns. *Science* **318**: 801–806.

696 **Bruno, L., Muto, A., Spadafora, N.D., Iaria, D., Chiappetta, A., Van Lijsebettens, M.,
697 and Bitonti, M.B.** (2011). Multi-probe in situ hybridization to whole mount Arabidopsis
698 seedlings. *Int. J. Dev. Biol.* **55**: 197–203.

699 **Chanvivattana, Y., Bishopp, A., Schubert, D., Stock, C., Moon, Y.-H., Sung, Z.R., and
700 Goodrich, J.** (2004). Interaction of Polycomb-group proteins controlling flowering in
701 Arabidopsis. *Development* **131**: 5263–5276.

702 **Ciferri, C., Lander, G.C., Maiolica, A., Herzog, F., Aebersold, R., and Nogales, E.**
703 (2012). Molecular architecture of human polycomb repressive complex 2. *Elife* **1**:
704 e00005.

705 **Clough, S.J. and Bent, A.F.** (1998). Floral dip: a simplified method for *Agrobacterium*-
706 mediated transformation of *Arabidopsis thaliana*. *The Plant Journal*.

707 **Coego, A., Brizuela, E., Castillejo, P., Ruíz, S., Koncz, C., Del Pozo, J.C., Pineiro, M.,
708 Jarillo, J.A., Paz-Ares, J., León, J., The TRANSPLANTA Consortium** (2014). The
709 TRANSPLANTA collection of Arabidopsis lines: a resource for functional analysis of
710 transcription factors based on their conditional overexpression. *The Plant Journal*.

711 **De Lucia, F., Crevillen, P., Jones, A.M.E., Greb, T., and Dean, C.** (2008). A PHD-
712 polycomb repressive complex 2 triggers the epigenetic silencing of FLC during
713 vernalization. *Proceedings of the National Academy of Sciences* **105**: 16831–16836.

714 **De Rybel, B. et al.** (2014). Integration of growth and patterning during vascular tissue
715 formation in Arabidopsis. *Science* **345**: 1255215–1255215.

716 **Deal, R.B. and Henikoff, S.** (2010). A Simple Method for Gene Expression and Chromatin
717 Profiling of Individual Cell Types within a Tissue. *Developmental Cell* **18**: 1030–1040.

- 718 **Deng, W., Buzas, D.M., Ying, H., Robertson, M., Taylor, J., Peacock, W.J., Dennis,**
719 **E.S., and Helliwell, C.** (2013). Arabidopsis Polycomb Repressive Complex 2 binding
720 sites contain putative GAGA factor binding motifs within coding regions of genes. *BMC*
721 *Genomics* **14**: 593.
- 722 **Derkacheva, M., Steinbach, Y., Wildhaber, T., Mozgová, I., Mahrez, W., Nanni, P.,**
723 **Bischof, S., Gruissem, W., and Hennig, L.** (2013). Arabidopsis MSI1 connects LHP1
724 to PRC2 complexes. *The EMBO Journal*.
- 725 **Dolan, L., Janmaat, K., Willemsen, V., Linstead, P., Poethig, S., Roberts, K., and**
726 **scheres, B.** (1993). Cellular organisation of the Arabidopsis thaliana root.
727 *Development* **119**: 71–84.
- 728 **Du, Z., Zhou, X., Ling, Y., Zhang, Z., and Su, Z.** (2010). agriGO: a GO analysis toolkit for
729 the agricultural community. *Nucleic Acids Res.* **38**: W64–70.
- 730 **Etchells, J.P. and Turner, S.R.** (2010). Orientation of vascular cell divisions in
731 Arabidopsis. *Plant Signal Behav* **5**: 730–732.
- 732 **Etchells, J.P., Provost, C.M., Mishra, L., and Turner, S.R.** (2013). WOX4 and WOX14
733 act downstream of the PXY receptor kinase to regulate plant vascular proliferation
734 independently of any role in vascular organisation. *Development* **140**: 2224–2234.
- 735 **Fasano, C.A., Dimos, J.T., Ivanova, N.B., Lowry, N., Lemischka, I.R., and Temple, S.**
736 (2007). shRNA knockdown of Bmi-1 reveals a critical role for p21-Rb pathway in NSC
737 self-renewal during development. *Cell Stem Cell* **1**: 87–99.
- 738 **Fisher, K. and Turner, S.** (2007). PXY, a receptor-like kinase essential for maintaining
739 polarity during plant vascular-tissue development. *Curr. Biol.* **17**: 1061–1066.
- 740 **Fu, C., Donovan, W.P., Shikapwashya-Hasser, O., Ye, X., and Cole, R.H.** (2014). Hot
741 Fusion: An Efficient Method to Clone Multiple DNA Fragments as Well as Inverted
742 Repeats without Ligase. *PLoS ONE* **9**: e115318.
- 743 **Gaudinier, A. et al.** (2011). Enhanced Y1H assays for Arabidopsis. *Nat Meth* **8**: 1053–
744 1055.
- 745 **Gu, X., Xu, T., and He, Y.** (2014). A histone H3 lysine-27 methyltransferase complex
746 represses lateral root formation in Arabidopsis thaliana. *Molecular Plant* **7**: 977–988.
- 747 **He, C., Chen, X., Huang, H., and Xu, L.** (2012). Reprogramming of H3K27me3 Is Critical
748 for Acquisition of Pluripotency from Cultured Arabidopsis Tissues. *PLoS Genet* **8**:
749 e1002911.
- 750 **Helin, K. and Dhanak, D.** (2013). Chromatin proteins and modifications as drug targets.
751 *Nature* **502**: 480–488.
- 752 **Hellens, R.P., Edwards, E.A., Leyland, N.R., Bean, S., and Mullineaux, P.M.** (2000).
753 pGreen: a versatile and flexible binary Ti vector for Agrobacterium-mediated plant
754 transformation. *Plant Mol Biol* **42**: 819–832.
- 755 **Hennig, L. and Derkacheva, M.** (2009). Diversity of Polycomb group complexes in plants:
756 same rules, different players? *Trends in Genetics* **25**: 414–423.

- 757 **Hennig, L., Taranto, P., Walser, M., Schönrock, N., and Grissem, W.** (2003).
758 Arabidopsis MS11 is required for epigenetic maintenance of reproductive development.
759 *Development* **130**: 2555–2565.
- 760 **Hirabayashi, Y., Suzuki, N., Tsuboi, M., Endo, T.A., Toyoda, T., Shinga, J., Koseki, H.,**
761 **Vidal, M., and Gotoh, Y.** (2009). Polycomb limits the neurogenic competence of
762 neural precursor cells to promote astrogenic fate transition. *Neuron* **63**: 600–613.
- 763 **Ikeuchi, M. et al.** (2015). PRC2 represses dedifferentiation of mature somatic cells in
764 Arabidopsis. *Nature Plants* **1**: 15089.
- 765 **Inoue, T., Higuchi, M., Hashimoto, Y., Seki, M., Kobayashi, M., Kato, T., Tabata, S.,**
766 **Shinozaki, K., and Kakimoto, T.** (2001). Identification of CRE1 as a cytokinin
767 receptor from Arabidopsis. *Nature* **409**: 1060–1063.
- 768 **Jullien, P.E., Mosquna, A., Ingouff, M., Sakata, T., Ohad, N., and Berger, F.** (2008).
769 Retinoblastoma and its binding partner MS11 control imprinting in Arabidopsis. *Plos*
770 *Biol* **6**: e194.
- 771 **Karimi, M., De Meyer, B., and Hilson, P.** (2005). Modular cloning in plant cells. *Trends in*
772 *Plant Science*.
- 773 **Kinoshita, T., Harada, J.J., Goldberg, R.B., and Fischer, R.L.** (2001). Polycomb
774 repression of flowering during early plant development. *Proc. Natl. Acad. Sci. U.S.A.*
775 **98**: 14156–14161.
- 776 **Kleer, C.G. et al.** (2003). EZH2 is a marker of aggressive breast cancer and promotes
777 neoplastic transformation of breast epithelial cells. *Proc. Natl. Acad. Sci. U.S.A.* **100**:
778 11606–11611.
- 779 **Köhler, C., Hennig, L., Bouveret, R., Gheyselinck, J., Grossniklaus, U., and Grissem,**
780 **W.** (2003). Arabidopsis MS11 is a component of the MEA/FIE Polycomb group complex
781 and required for seed development. *The EMBO Journal* **22**: 4804–4814.
- 782 **Köhler, C., Page, D.R., Gagliardini, V., and Grossniklaus, U.** (2005). The Arabidopsis
783 thaliana MEDEA Polycomb group protein controls expression of PHERES1 by parental
784 imprinting. *Nat Genet* **37**: 28–30.
- 785 **Kubo, M.** (2005). Transcription switches for protoxylem and metaxylem vessel formation.
786 *Genes & Development* **19**: 1855–1860.
- 787 **Kumar, R., Ichihashi, Y., Kimura, S., Chitwood, D.H., Headland, L.R., Peng, J., Maloof,**
788 **J.N., and Sinha, N.R.** (2012). A high-throughput method for Illumina RNA-Seq library
789 preparation. *Front Plant Sci* **3**.
- 790 **Kuzmichev, A., Margueron, R., Vaquero, A., Preissner, T.S., Scher, M., Kirmizis, A.,**
791 **Ouyang, X., Brockdorff, N., Abate-Shen, C., Farnham, P., and Reinberg, D.** (2005).
792 Composition and histone substrates of polycomb repressive group complexes change
793 during cellular differentiation. *Proc. Natl. Acad. Sci. U.S.A.* **102**: 1859–1864.
- 794 **Lafos, M., Kroll, P., Hohenstatt, M.L., Thorpe, F.L., Clarenz, O., and Schubert, D.**
795 (2011). Dynamic regulation of H3K27 trimethylation during Arabidopsis differentiation.
796 *PLoS Genet* **7**: e1002040.

- 797 **Langmead, B., Trapnell, C., Pop, M., and Salzberg, S.L.** (2009). Ultrafast and memory-
798 efficient alignment of short DNA sequences to the human genome. *Genome Biol* **10**:
799 R25.
- 800 **Laugesen, A. and Helin, K.** (2014). Chromatin repressive complexes in stem cells,
801 development, and cancer. *Cell Stem Cell* **14**: 735–751.
- 802 **Lee, J.-Y., Colinas, J., Wang, J.Y., Mace, D., Ohler, U., and Benfey, P.N.** (2006).
803 Transcriptional and posttranscriptional regulation of transcription factor expression in
804 *Arabidopsis* roots. *Proc. Natl. Acad. Sci. U.S.A.* **103**: 6055–6060.
- 805 **Ma, S., Shah, S., Bohnert, H.J., Snyder, M., and Dinesh-Kumar, S.P.** (2013).
806 Incorporating motif analysis into gene co-expression networks reveals novel modular
807 expression pattern and new signaling pathways. *PLoS Genet* **9**: e1003840.
- 808 **Mahonen, A.P.** (2000). A novel two-component hybrid molecule regulates vascular
809 morphogenesis of the *Arabidopsis* root. *Genes & Development* **14**: 2938–2943.
- 810 **Mahonen, A.P.** (2006). Cytokinin Signaling and Its Inhibitor AHP6 Regulate Cell Fate
811 During Vascular Development. *Science* **311**: 94–98.
- 812 **Mallory, A.C.** (2005). MicroRNA-Directed Regulation of *Arabidopsis* AUXIN RESPONSE
813 FACTOR17 Is Essential for Proper Development and Modulates Expression of Early
814 Auxin Response Genes. *THE PLANT CELL ONLINE* **17**: 1360–1375.
- 815 **Margueron, R. and Reinberg, D.** (2011). The Polycomb complex PRC2 and its mark in
816 life. *Nature* **469**: 343–349.
- 817 **Margueron, R., Li, G., Sarma, K., Blais, A., Zavadil, J., Woodcock, C.L., Dynlacht,
818 B.D., and Reinberg, D.** (2008). Ezh1 and Ezh2 maintain repressive chromatin through
819 different mechanisms. *Molecular Cell* **32**: 503–518.
- 820 **Mozgová, I. and Hennig, L.** (2015). The Polycomb Group Protein Regulatory Network.
821 <http://dx.doi.org/10.1146/annurev-arplant-043014-115627>.
- 822 **Nakagawa, T., Kurose, T., Hino, T., Tanaka, K., Kawamukai, M., Niwa, Y., Toyooka, K.,
823 Matsuoka, K., Jinbo, T., and Kimura, T.** (2007). Development of series of gateway
824 binary vectors, pGWBs, for realizing efficient construction of fusion genes for plant
825 transformation. *J. Biosci. Bioeng.* **104**: 34–41.
- 826 **Ohno, K., McCabe, D., Czermin, B., Imhof, A., and Pirrotta, V.** (2008). ESC, ESCL and
827 their roles in Polycomb Group mechanisms. *Mech. Dev.* **125**: 527–541.
- 828 **Okushima, Y.** (2005). Functional Genomic Analysis of the AUXIN RESPONSE FACTOR
829 Gene Family Members in *Arabidopsis thaliana*: Unique and Overlapping Functions of
830 ARF7 and ARF19. *The Plant Cell* **17**: 444–463.
- 831 **Ossowski, S., Schwab, R., and Weigel, D.** (2008). Gene silencing in plants using artificial
832 microRNAs and other small RNAs. *The Plant Journal* **53**: 674–690.
- 833 **Pasini, D., Bracken, A.P., Hansen, J.B., Capillo, M., and Helin, K.** (2007). The
834 polycomb group protein Suz12 is required for embryonic stem cell differentiation. *Mol.*
835 *Cell. Biol.* **27**: 3769–3779.

- 836 **Quinlan, A.R. and Hall, I.M.** (2010). BEDTools: a flexible suite of utilities for comparing
837 genomic features. *Bioinformatics* **26**: 841–842.
- 838 **Rademacher, E.H., Möller, B., Lokerse, A.S., Llavata-Peris, C.I., van den Berg, W.,**
839 **and Weijers, D.** (2011). A cellular expression map of the Arabidopsis AUXIN
840 RESPONSE FACTOR gene family. *The Plant Journal* **68**: 597–606.
- 841 **Reece-Hoyes, J.S. et al.** (2011). Yeast one-hybrid assays for gene-centered human gene
842 regulatory network mapping. *Nat Meth* **8**: 1050–1052.
- 843 **Roudier, F. et al.** (2011). Integrative epigenomic mapping defines four main chromatin
844 states in Arabidopsis. *The EMBO Journal* **30**: 1928–1938.
- 845 **Rueda-Romero, P., Barrero-Sicilia, C., Gómez-Cadenas, A., Carbonero, P., and**
846 **Oñate-Sánchez, L.** (2012). Arabidopsis thaliana DOF6 negatively affects germination
847 in non-after-ripened seeds and interacts with TCP14. *Journal of Experimental Botany*
848 **63**: 1937–1949.
- 849 **Scheres, B.** (2007). Stem-cell niches: nursery rhymes across kingdoms. *Nature Reviews*
850 *Molecular Cell Biology* **8**: 345–354.
- 851 **Shahram Emami, M.-C.Y.J.R.D.** (2013). A robust family of Golden Gate Agrobacterium
852 vectors for plant synthetic biology. *Front Plant Sci* **4**.
- 853 **Shannon, P., Markiel, A., Ozier, O., Baliga, N.S., Wang, J.T., Ramage, D., Amin, N.,**
854 **Schwikowski, B., and Ideker, T.** (2003). Cytoscape: a software environment for
855 integrated models of biomolecular interaction networks. *Genome Research* **13**: 2498–
856 2504.
- 857 **She, W., Grimanelli, D., and Baroux, C.** (2014). An efficient method for quantitative,
858 single-cell analysis of chromatin modification and nuclear architecture in whole-mount
859 ovules in Arabidopsis. *J Vis Exp*: e51530.
- 860 **Sher, F., Rössler, R., Brouwer, N., Balasubramaniyan, V., Boddeke, E., and Copray, S.**
861 (2008). Differentiation of neural stem cells into oligodendrocytes: involvement of the
862 polycomb group protein Ezh2. *Stem Cells* **26**: 2875–2883.
- 863 **Sieburth, L.E. and Meyerowitz, E.M.** (1997). Molecular dissection of the AGAMOUS
864 control region shows that cis elements for spatial regulation are located intragenically.
865 *The Plant Cell* **9**: 355–365.
- 866 **Stojic, L. et al.** (2011). Chromatin regulated interchange between polycomb repressive
867 complex 2 (PRC2)-Ezh2 and PRC2-Ezh1 complexes controls myogenin activation in
868 skeletal muscle cells. *Epigenetics Chromatin* **4**: 16.
- 869 **Takawa, M. et al.** (2011). Validation of the histone methyltransferase EZH2 as a
870 therapeutic target for various types of human cancer and as a prognostic marker.
871 *Cancer Sci.* **102**: 1298–1305.
- 872 **Taylor-Teeples, M. et al.** (2015). An Arabidopsis gene regulatory network for secondary
873 cell wall synthesis. *Nature* **517**: 571–575.
- 874 **Terpstra, I. and Heidstra, R.** (2009). Stem cells: The root of all cells. *Seminars in Cell &*

- 875 Developmental Biology **20**: 1089–1096.
- 876 **Truernit, E., Bauby, H., Dubreucq, B., Grandjean, O., Runions, J., Barthelemy, J., and**
877 **Palauqui, J.C.** (2008). High-Resolution Whole-Mount Imaging of Three-Dimensional
878 Tissue Organization and Gene Expression Enables the Study of Phloem Development
879 and Structure in Arabidopsis. THE PLANT CELL ONLINE **20**: 1494–1503.
- 880 **Turck, F., Roudier, F., Farrona, S., Martin-Magniette, M.-L., Guillaume, E., Buisine, N.,**
881 **Gagnot, S., Martienssen, R.A., Coupland, G., and Colot, V.** (2007). Arabidopsis
882 TFL2/LHP1 specifically associates with genes marked by trimethylation of histone H3
883 lysine 27. PLoS Genet **3**: e86.
- 884 **Varambally, S., Dhanasekaran, S.M., Zhou, M., Barrette, T.R., Kumar-Sinha, C.,**
885 **Sanda, M.G., Ghosh, D., Pienta, K.J., Sewalt, R.G.A.B., Otte, A.P., Rubin, M.A.,**
886 **and Chinnaiyan, A.M.** (2002). The polycomb group protein EZH2 is involved in
887 progression of prostate cancer. Nature **419**: 624–629.
- 888 **Wagener, N., Macher-Goeppinger, S., Pritsch, M., Hüsing, J., Hoppe-Seyler, K.,**
889 **Schirmacher, P., Pfitzenmaier, J., Haferkamp, A., Hoppe-Seyler, F., and**
890 **Hohenfellner, M.** (2010). Enhancer of zeste homolog 2 (EZH2) expression is an
891 independent prognostic factor in renal cell carcinoma. BMC Cancer **10**: 524.
- 892 **Wang, D., Tyson, M.D., Jackson, S.S., and Yadegari, R.** (2006). Partially redundant
893 functions of two SET-domain polycomb-group proteins in controlling initiation of seed
894 development in Arabidopsis. Proc. Natl. Acad. Sci. U.S.A. **103**: 13244–13249.
- 895 **Yadegari, R., Kinoshita, T., Lotan, O., Cohen, G., Katz, A., Choi, Y., Katz, A.,**
896 **Nakashima, K., Harada, J.J., Goldberg, R.B., Fischer, R.L., and Ohad, N.** (2000).
897 Mutations in the FIE and MEA genes that encode interacting polycomb proteins cause
898 parent-of-origin effects on seed development by distinct mechanisms. The Plant Cell
899 **12**: 2367–2382.
- 900 **Yamaguchi, M., Ohtani, M., Mitsuda, N., Kubo, M., Ohme-Takagi, M., Fukuda, H., and**
901 **Demura, T.** (2010). VND-INTERACTING2, a NAC domain transcription factor,
902 negatively regulates xylem vessel formation in Arabidopsis. THE PLANT CELL
903 ONLINE **22**: 1249–1263.
- 904 **Zhang, X., Clarenz, O., Cokus, S., Bernatavichute, Y.V., Pellegrini, M., Goodrich, J.,**
905 **and Jacobsen, S.E.** (2007a). Whole-genome analysis of histone H3 lysine 27
906 trimethylation in Arabidopsis. Plos Biol **5**: e129.
- 907 **Zhang, X., Germann, S., Blus, B.J., Khorasanizadeh, S., Gaudin, V., and Jacobsen,**
908 **S.E.** (2007b). The Arabidopsis LHP1 protein colocalizes with histone H3 Lys27
909 trimethylation. Nat. Struct. Mol. Biol. **14**: 869–871.

910

911 **FIGURE LEGENDS**

912 **Figure 1.** PRC2 genes are expressed in unique and overlapping cell types in the
913 *Arabidopsis thaliana* root. For each genotype, the top panel shows the root meristem
914 while the bottom panel shows the maturation/differentiation zone of the root. All images

915 were taken under the same acquisition conditions. **(A)** VRN2_{pro}:GUS expression. **(B)**
916 EMF2_{pro}:GUS expression. **(C)** FIS2_{pro}:GUS expression. **(D)** SWN_{pro}:GUS expression. **(E)**
917 CLF_{pro}:VenusN7 expression. **(F)** MEA_{pro}:GUS expression. **(G)** FIE_{pro}:GUS expression. **(H)**
918 MSI1_{pro}:GUS expression. **(I)** Cartoon of the different cell types and tissues in the
919 *Arabidopsis thaliana* root. **(J)** Promoter lengths of the different PRC2 genes used in the
920 reporter lines . Translational start site = TSS.

921 **Figure 2:** PRC2 proteins are found in unique and overlapping cell types in the *Arabidopsis*
922 *thaliana* root. For each genotype, the left panel shows the root meristem while the right
923 panel shows the maturation/differentiation zone of the root. (A) VRN2_{pro}:VRN2:GUS (B)
924 EMF2_{pro}:EMF2:GFP (C) SWN_{pro}:SWN:GFP (D) MEA_{pro}:MEA:YFP in *mea-3* (E)
925 CLF_{pro}:CFP:gCLF in *clf-29*, F) MSI1_{pro}:MSI1:GFP (G) FIE_{pro}:FIE:GFP in *fie-1*.

926 **Figure 3:** PRC2 regulates cell proliferation in the root meristem and vascular cylinder. **(A-**
927 **B)** Whole mount immunostaining with antibodies specific for H3K27me3 (green in the wild-
928 type Col-0) **(A)** and in the *clf-28 swn-7* double mutant **(B)**. Nuclear staining is indicated
929 with white arrows. A magnified nucleus is shown in the inset. **(C-D)** Differential
930 Interference Contrast image of the root meristem of the wild-type Col-0 **(C)** and the *clf-28*
931 *swn-7* double mutant **(D)**. White lines indicate the root meristematic zone (MZ). **(E-H)**
932 Cross-sections showing the root vascular cylinder in wild-type Col-0 **(E)**, *clf-28 swn-7* **(F)**,
933 *fie042* **(G)**, and in the WOL_{pro}:amiRNA_MSI line **(H)**. Green indicates pericycle cells,
934 purple indicates procambium cells, red/orange indicates phloem cells. **(I-J)** The MSI
935 protein is expressed ubiquitously throughout the *Arabidopsis thaliana* root **(I)** but is
936 depleted specifically from the vascular cylinder in the WOL_{pro}:amiRNA_MSI1 line in the
937 MSI1_{pro}:MSI1:GFP background (white arrows with one head) **(J)**. Note the reduction in the
938 length of the root meristem (white arrow with two heads). **(K-L)** Differential interference
939 contrast image showing two protoxylem pole cell files (black asterisk) in the wild-type Col-0
940 **(L)** and ectopic protoxylem (black asterisk) and metaxylem (blue asterisk) in the *fie042*
941 mutant background **(L)**. **(M)** There are significantly more procambium and phloem and
942 epidermal cells in the *clf-28 swn-7* mutant compared to wild-type Col-0. The reduction in
943 *MSI1* expression shows increased number of cortical and endodermal cells but lower
944 levels of cells in the stele. **(N)** The roots of *swn-7*, *clf-28 swn-7* and WOL_{pro}:amiRNA_MSI
945 are significantly shorter than wild type Col-0 and *clf-29*. **(O)** There are more cells in the
946 meristem of *clf-29* and fewer in *clf-28 swn-7* and WOL_{pro}:amiRNA_MSI relative to wild type
947 (Col-0). In all cases, significance was tested using a t-test. * = p<.05; ** = p<.01; *** =
948 p<.001. Error bars indicate the standard error value.

949 **Figure 4.** PRC2 regulates the balance between cell proliferation and differentiation in a
950 tissue-specific manner in the *Arabidopsis thaliana* root. **(A)** Expression levels of genes
951 marked by H3K27me3 in vascular cells relative to expression levels of genes marked by
952 H3K4me3. Whole root and vascular-specific (pWOL:GFP positive) root protoplast were
953 isolated by FACS and H3K27me3/H3K4me3 enriched regions were resolved by ChIPseq.
954 Expression of the vascular specific H3K27me3 and H3K4me3 marked genes was
955 determined using Brady et al. 2007 transcriptional data. **(B)** Number of genes marked by
956 H3K27me3 in non-vascular cells. **(C-F)** Expression of a gene marked specifically by
957 H3K27me3 and not expressed in vascular cells **(C,D)** ARF17_{pro}:GFP and of a gene
958 marked specifically by H3K27me3 and not expressed in non-vascular cells VND7_{pro}:nYFP
959 **(E,F)**. **(G-J)** Estradiol induction of the ARF17 transcription factor results in small regions of
960 additional cell proliferation in the vascular cylinder **(I,J)** compared to the mock-treated root
961 **(G,H)**. Asterisks indicate ectopic cell proliferation. **(K-L)** Estradiol induction of the VND7
962 transcription factor **(L)** results in ectopic xylem cell differentiation compared to a mock-
963 treated root **(K)**.

964 **Figure 5.** Transcription factors regulating PRC2 gene expression *in planta*. Squares
965 represent PRC2 gene promoters, circles represent transcription factors. A line between a
966 transcription factor and promoter indicates that an interaction was observed by yeast one
967 hybrid. A green line or a red line indicates that the transcription factor has been validated
968 *in planta* as activating or repressing, respectively, the target gene *in planta* in either a
969 trans-activation assay or upon B-estradiol induction of the transcription factor.
970 Transcription factors are additionally colored according to their respective family.
971 Transcription factors that interact with the most PRC2 gene promoters are indicated at the
972 top of the network, while transcription factors that interact with just a single promoter are
973 located just beside their respective PRC2 gene promoter. Network information is available
974 in Supplemental Data Set 1.

975 **Figure 6.** Functional validation of a multi-tier PRC2 gene regulatory network (TF → PRC2
976 gene → H3K27me3 regulated gene). **(A)** β-estradiol induction (3 days) of the DOF6
977 transcription factor results in a significantly shorter root. Root inhibition caused by the
978 induction of DOF6 is abolished in the *clf29* background. **(B)** ARF17 expression is activated
979 in the *clf-29* mutant. **(C)** Induction of DOF6 results in a significant increase in the amount
980 of CLF expression and a corresponding repression of ARF17 expression, as revealed by
981 RT-qPCR. **(D)** Induction of DOF6 results in a significant increase in H3K27me3 deposition
982 in the ARF17 loci in the root tissue. **(E)** DOF6 induction does not affect ARF17 expression

983 in the *clf-29* background. (F) Whole mount in-situ hybridization of *ARF17* mRNA. *ARF17*
984 expression domain is expanded towards the vascular cylinder in the *clf-29* mutant. In all
985 cases significance was tested using a t-test. * = $p < .05$; ** = $p < .01$; *** = $p < .001$. Error bars
986 represent the standard error value of the \log_2 transformed expression. The mean is from 3
987 independent experiments (biological replicates), calculated from the average of 3 technical
988 replicates per biological replicate. Each biological replicate captures expression from
989 approximately 200 roots of each respective genotype. In each case, the $\Delta\Delta\text{Ct}$ was
990 calculated relative to an ubiquitin10 control.

991

Parsed Citations

Aichinger, E., Villar, C.B.R., Di Mambro, R., Sabatini, S., and Kohler, C. (2011). The CHD3 Chromatin Remodeler PICKLE and Polycomb Group Proteins Antagonistically Regulate Meristem Activity in the Arabidopsis Root. *The Plant Cell* 23: 1047-1060.

Pubmed: [Author and Title](#)

CrossRef: [Author and Title](#)

Google Scholar: [Author Only](#) [Title Only](#) [Author and Title](#)

Aichinger, E., Villar, C.B.R., Farrona, S., Reyes, J.C., Hennig, L., and Köhler, C. (2009). CHD3 Proteins and Polycomb Group Proteins Antagonistically Determine Cell Identity in Arabidopsis. *PLoS Genet* 5: e1000605.

Pubmed: [Author and Title](#)

CrossRef: [Author and Title](#)

Google Scholar: [Author Only](#) [Title Only](#) [Author and Title](#)

Aldiri, I. and Vetter, M.L. (2009). Characterization of the expression pattern of the PRC2 core subunit Suz12 during embryonic development of *Xenopus laevis*. *Dev. Dyn.* 238: 3185-3192.

Pubmed: [Author and Title](#)

CrossRef: [Author and Title](#)

Google Scholar: [Author Only](#) [Title Only](#) [Author and Title](#)

Bemer, M. and Grossniklaus, U. (2012). Dynamic regulation of Polycomb group activity during plant development. *Curr. Opin. Plant Biol.* 15: 523-529.

Pubmed: [Author and Title](#)

CrossRef: [Author and Title](#)

Google Scholar: [Author Only](#) [Title Only](#) [Author and Title](#)

Benfey, P.N. and scheres, B. (2000). Root development. *Curr. Biol.* 10: R813-5.

Pubmed: [Author and Title](#)

CrossRef: [Author and Title](#)

Google Scholar: [Author Only](#) [Title Only](#) [Author and Title](#)

Birnbaum, K., Shasha, D.E., Wang, J.Y., and Jung, J.W. (2003). A gene expression map of the Arabidopsis root. *Science*.

Pubmed: [Author and Title](#)

CrossRef: [Author and Title](#)

Google Scholar: [Author Only](#) [Title Only](#) [Author and Title](#)

Bouyer, D., Roudier, F., Heese, M., Andersen, E.D., Gey, D., Nowack, M.K., Goodrich, J., Renou, J.-P., Grini, P.E., Colot, V., and Schnittger, A. (2011). Polycomb Repressive Complex 2 Controls the Embryo-to-Seedling Phase Transition. *PLoS Genet* 7: e1002014.

Pubmed: [Author and Title](#)

CrossRef: [Author and Title](#)

Google Scholar: [Author Only](#) [Title Only](#) [Author and Title](#)

Bracken, A.P., Pasini, D., Capra, M., Prosperini, E., Colli, E., and Helin, K. (2003). EZH2 is downstream of the pRB-E2F pathway, essential for proliferation and amplified in cancer. *The EMBO Journal* 22: 5323-5335.

Pubmed: [Author and Title](#)

CrossRef: [Author and Title](#)

Google Scholar: [Author Only](#) [Title Only](#) [Author and Title](#)

Brady, S.M. et al. (2011). A stele-enriched gene regulatory network in the Arabidopsis root. *Molecular Systems Biology* 7: 459.

Pubmed: [Author and Title](#)

CrossRef: [Author and Title](#)

Google Scholar: [Author Only](#) [Title Only](#) [Author and Title](#)

Brady, S.M., Orlando, D.A., Lee, J.Y., Wang, J.Y., Koch, J., Dinneny, J.R., Mace, D., Ohler, U., and Benfey, P.N. (2007). A High-Resolution Root Spatiotemporal Map Reveals Dominant Expression Patterns. *Science* 318: 801-806.

Pubmed: [Author and Title](#)

CrossRef: [Author and Title](#)

Google Scholar: [Author Only](#) [Title Only](#) [Author and Title](#)

Bruno, L., Muto, A., Spadafora, N.D., Iaria, D., Chiappetta, A., Van Lijsebettens, M., and Bitonti, M.B. (2011). Multi-probe in situ hybridization to whole mount Arabidopsis seedlings. *Int. J. Dev. Biol.* 55: 197-203.

Pubmed: [Author and Title](#)

CrossRef: [Author and Title](#)

Google Scholar: [Author Only](#) [Title Only](#) [Author and Title](#)

Chanvivattana, Y., Bishopp, A., Schubert, D., Stock, C., Moon, Y.-H., Sung, Z.R., and Goodrich, J. (2004). Interaction of Polycomb-group proteins controlling flowering in Arabidopsis. *Development* 131: 5263-5276.

Pubmed: [Author and Title](#)

CrossRef: [Author and Title](#)

Google Scholar: [Author Only](#) [Title Only](#) [Author and Title](#)

Ciferri, C., Lander, G.C., Maiolica, A., Herzog, F., Aebersold, R., and Nogales, E. (2012). Molecular architecture of human polycomb repressive complex 2. *Elife* 1: e00005.

Pubmed: [Author and Title](#)

CrossRef: [Author and Title](#)

Google Scholar: [Author Only](#) [Title Only](#) [Author and Title](#)

Clough, S.J. and Bent, A.F. (1998). Floral dip: a simplified method for Agrobacterium-mediated transformation of Arabidopsis thaliana. *The Plant Journal*.

Pubmed: [Author and Title](#)
CrossRef: [Author and Title](#)
Google Scholar: [Author Only](#) [Title Only](#) [Author and Title](#)

Coego, A, Brizuela, E., Castillejo, P., Ruiz, S., Koncz, C., Del Pozo, J.C., Pineiro, M., Jarillo, J.A, Paz-Ares, J., León, J., The TRANSPLANTA Consortium (2014). The TRANSPLANTA collection of Arabidopsis lines: a resource for functional analysis of transcription factors based on their conditional overexpression. The Plant Journal.

Pubmed: [Author and Title](#)
CrossRef: [Author and Title](#)
Google Scholar: [Author Only](#) [Title Only](#) [Author and Title](#)

De Lucia, F., Crevillen, P., Jones, A.M.E., Greb, T., and Dean, C. (2008). A PHD-polycomb repressive complex 2 triggers the epigenetic silencing of FLC during vernalization. Proceedings of the National Academy of Sciences 105: 16831-16836.

Pubmed: [Author and Title](#)
CrossRef: [Author and Title](#)
Google Scholar: [Author Only](#) [Title Only](#) [Author and Title](#)

De Rybel, B. et al. (2014). Integration of growth and patterning during vascular tissue formation in Arabidopsis. Science 345: 1255215-1255215.

Pubmed: [Author and Title](#)
CrossRef: [Author and Title](#)
Google Scholar: [Author Only](#) [Title Only](#) [Author and Title](#)

Deal, R.B. and Henikoff, S. (2010). A Simple Method for Gene Expression and Chromatin Profiling of Individual Cell Types within a Tissue. Developmental Cell 18: 1030-1040.

Pubmed: [Author and Title](#)
CrossRef: [Author and Title](#)
Google Scholar: [Author Only](#) [Title Only](#) [Author and Title](#)

Deng, W., Buzas, D.M., Ying, H., Robertson, M., Taylor, J., Peacock, W.J., Dennis, E.S., and Helliwell, C. (2013). Arabidopsis Polycomb Repressive Complex 2 binding sites contain putative GAGA factor binding motifs within coding regions of genes. BMC Genomics 14: 593.

Pubmed: [Author and Title](#)
CrossRef: [Author and Title](#)
Google Scholar: [Author Only](#) [Title Only](#) [Author and Title](#)

Derkacheva, M., Steinbach, Y., Wildhaber, T., Mozhová, I., Mahrez, W., Nanni, P., Bischof, S., Grisse, W., and Hennig, L. (2013). Arabidopsis MSI1 connects LHP1 to PRC2 complexes. The EMBO Journal.

Pubmed: [Author and Title](#)
CrossRef: [Author and Title](#)
Google Scholar: [Author Only](#) [Title Only](#) [Author and Title](#)

Dolan, L., Janmaat, K., Willemsen, V., Linstead, P., Poethig, S., Roberts, K., and scheres, B. (1993). Cellular organisation of the Arabidopsis thaliana root. Development 119: 71-84.

Pubmed: [Author and Title](#)
CrossRef: [Author and Title](#)
Google Scholar: [Author Only](#) [Title Only](#) [Author and Title](#)

Du, Z., Zhou, X., Ling, Y., Zhang, Z., and Su, Z. (2010). agriGO: a GO analysis toolkit for the agricultural community. Nucleic Acids Res. 38: W64-70.

Pubmed: [Author and Title](#)
CrossRef: [Author and Title](#)
Google Scholar: [Author Only](#) [Title Only](#) [Author and Title](#)

Etchells, J.P. and Turner, S.R. (2010). Orientation of vascular cell divisions in Arabidopsis. Plant Signal Behav 5: 730-732.

Pubmed: [Author and Title](#)
CrossRef: [Author and Title](#)
Google Scholar: [Author Only](#) [Title Only](#) [Author and Title](#)

Etchells, J.P., Provost, C.M., Mishra, L., and Turner, S.R. (2013). WOX4 and WOX14 act downstream of the PXY receptor kinase to regulate plant vascular proliferation independently of any role in vascular organisation. Development 140: 2224-2234.

Pubmed: [Author and Title](#)
CrossRef: [Author and Title](#)
Google Scholar: [Author Only](#) [Title Only](#) [Author and Title](#)

Fasano, C.A., Dimos, J.T., Ivanova, N.B., Lowry, N., Lemischka, I.R., and Temple, S. (2007). shRNA knockdown of Bmi-1 reveals a critical role for p21-Rb pathway in NSC self-renewal during development. Cell Stem Cell 1: 87-99.

Pubmed: [Author and Title](#)
CrossRef: [Author and Title](#)
Google Scholar: [Author Only](#) [Title Only](#) [Author and Title](#)

Fisher, K. and Turner, S. (2007). PXY, a receptor-like kinase essential for maintaining polarity during plant vascular-tissue development. Curr. Biol. 17: 1061-1066.

Pubmed: [Author and Title](#)
CrossRef: [Author and Title](#)
Google Scholar: [Author Only](#) [Title Only](#) [Author and Title](#)

Fu, C., Donovan, W.P., Shikapwashya-Hasser, O., Ye, X., and Cole, R.H. (2014). Hot Fusion: An Efficient Method to Clone Multiple DNA Fragments as Well as Inverted Repeats without Ligase. PLoS ONE 9: e115318.

Pubmed: [Author and Title](#)

CrossRef: [Author and Title](#)
Google Scholar: [Author Only Title Only Author and Title](#)

Gaudinier, A. et al. (2011). Enhanced Y1H assays for Arabidopsis. Nat Meth 8: 1053-1055.

Pubmed: [Author and Title](#)
CrossRef: [Author and Title](#)
Google Scholar: [Author Only Title Only Author and Title](#)

Gu, X., Xu, T., and He, Y. (2014). A histone H3 lysine-27 methyltransferase complex represses lateral root formation in Arabidopsis thaliana. Molecular Plant 7: 977-988.

Pubmed: [Author and Title](#)
CrossRef: [Author and Title](#)
Google Scholar: [Author Only Title Only Author and Title](#)

He, C., Chen, X., Huang, H., and Xu, L. (2012). Reprogramming of H3K27me3 Is Critical for Acquisition of Pluripotency from Cultured Arabidopsis Tissues. PLoS Genet 8: e1002911.

Pubmed: [Author and Title](#)
CrossRef: [Author and Title](#)
Google Scholar: [Author Only Title Only Author and Title](#)

Helin, K. and Dhanak, D. (2013). Chromatin proteins and modifications as drug targets. Nature 502: 480-488.

Pubmed: [Author and Title](#)
CrossRef: [Author and Title](#)
Google Scholar: [Author Only Title Only Author and Title](#)

Hellens, R.P., Edwards, E.A., Leyland, N.R., Bean, S., and Mullineaux, P.M. (2000). pGreen: a versatile and flexible binary Ti vector for Agrobacterium-mediated plant transformation. Plant Mol Biol 42: 819-832.

Pubmed: [Author and Title](#)
CrossRef: [Author and Title](#)
Google Scholar: [Author Only Title Only Author and Title](#)

Hennig, L. and Derkacheva, M. (2009). Diversity of Polycomb group complexes in plants: same rules, different players? Trends in Genetics 25: 414-423.

Pubmed: [Author and Title](#)
CrossRef: [Author and Title](#)
Google Scholar: [Author Only Title Only Author and Title](#)

Hennig, L., Taranto, P., Walsler, M., Schönrock, N., and Gruißem, W. (2003). Arabidopsis MSI1 is required for epigenetic maintenance of reproductive development. Development 130: 2555-2565.

Pubmed: [Author and Title](#)
CrossRef: [Author and Title](#)
Google Scholar: [Author Only Title Only Author and Title](#)

Hirabayashi, Y., Suzuki, N., Tsuboi, M., Endo, T.A., Toyoda, T., Shinga, J., Koseki, H., Vidal, M., and Gotoh, Y. (2009). Polycomb limits the neurogenic competence of neural precursor cells to promote astrogenic fate transition. Neuron 63: 600-613.

Pubmed: [Author and Title](#)
CrossRef: [Author and Title](#)
Google Scholar: [Author Only Title Only Author and Title](#)

Ikeuchi, M. et al. (2015). PRC2 represses dedifferentiation of mature somatic cells in Arabidopsis. Nature Plants 1: 15089.

Pubmed: [Author and Title](#)
CrossRef: [Author and Title](#)
Google Scholar: [Author Only Title Only Author and Title](#)

Inoue, T., Higuchi, M., Hashimoto, Y., Seki, M., Kobayashi, M., Kato, T., Tabata, S., Shinozaki, K., and Kakimoto, T. (2001). Identification of CRE1 as a cytokinin receptor from Arabidopsis. Nature 409: 1060-1063.

Pubmed: [Author and Title](#)
CrossRef: [Author and Title](#)
Google Scholar: [Author Only Title Only Author and Title](#)

Jullien, P.E., Mosquna, A., Ingouff, M., Sakata, T., Ohad, N., and Berger, F. (2008). Retinoblastoma and its binding partner MSI1 control imprinting in Arabidopsis. Plos Biol 6: e194.

Pubmed: [Author and Title](#)
CrossRef: [Author and Title](#)
Google Scholar: [Author Only Title Only Author and Title](#)

Karimi, M., De Meyer, B., and Hilson, P. (2005). Modular cloning in plant cells. Trends in Plant Science.

Pubmed: [Author and Title](#)
CrossRef: [Author and Title](#)
Google Scholar: [Author Only Title Only Author and Title](#)

Kinoshita, T., Harada, J.J., Goldberg, R.B., and Fischer, R.L. (2001). Polycomb repression of flowering during early plant development. Proc. Natl. Acad. Sci. U.S.A 98: 14156-14161.

Pubmed: [Author and Title](#)
CrossRef: [Author and Title](#)
Google Scholar: [Author Only Title Only Author and Title](#)

Kleer, C.G. et al. (2003). EZH2 is a marker of aggressive breast cancer and promotes neoplastic transformation of breast epithelial cells. Proc. Natl. Acad. Sci. U.S.A 100: 11606-11611.

Pubmed: [Author and Title](#)
CrossRef: [Author and Title](#)

Google Scholar: [Author Only](#) [Title Only](#) [Author and Title](#)

Köhler, C., Hennig, L., Bouveret, R., Gheyselinck, J., Grossniklaus, U., and Grissem, W. (2003). Arabidopsis MSI1 is a component of the MEA/FIE Polycomb group complex and required for seed development. The EMBO Journal 22: 4804-4814.

Pubmed: [Author and Title](#)

CrossRef: [Author and Title](#)

Google Scholar: [Author Only](#) [Title Only](#) [Author and Title](#)

Köhler, C., Page, D.R., Gagliardini, V., and Grossniklaus, U. (2005). The Arabidopsis thaliana MEDEA Polycomb group protein controls expression of PHERES1 by parental imprinting. Nat Genet 37: 28-30.

Pubmed: [Author and Title](#)

CrossRef: [Author and Title](#)

Google Scholar: [Author Only](#) [Title Only](#) [Author and Title](#)

Kubo, M. (2005). Transcription switches for protoxylem and metaxylem vessel formation. Genes & Development 19: 1855-1860.

Pubmed: [Author and Title](#)

CrossRef: [Author and Title](#)

Google Scholar: [Author Only](#) [Title Only](#) [Author and Title](#)

Kumar, R., Ichihashi, Y., Kimura, S., Chitwood, D.H., Headland, L.R., Peng, J., Maloof, J.N., and Sinha, N.R. (2012). A high-throughput method for Illumina RNA-Seq library preparation. Front Plant Sci 3.

Pubmed: [Author and Title](#)

CrossRef: [Author and Title](#)

Google Scholar: [Author Only](#) [Title Only](#) [Author and Title](#)

Kuzmichev, A., Margueron, R., Vaquero, A., Preissner, T.S., Scher, M., Kirmizis, A., Ouyang, X., Brockdorff, N., Abate-Shen, C., Farnham, P., and Reinberg, D. (2005). Composition and histone substrates of polycomb repressive group complexes change during cellular differentiation. Proc. Natl. Acad. Sci. U.S.A. 102: 1859-1864.

Pubmed: [Author and Title](#)

CrossRef: [Author and Title](#)

Google Scholar: [Author Only](#) [Title Only](#) [Author and Title](#)

Lafos, M., Kroll, P., Hohenstatt, M.L., Thorpe, F.L., Clarenz, O., and Schubert, D. (2011). Dynamic regulation of H3K27 trimethylation during Arabidopsis differentiation. PLoS Genet 7: e1002040.

Pubmed: [Author and Title](#)

CrossRef: [Author and Title](#)

Google Scholar: [Author Only](#) [Title Only](#) [Author and Title](#)

Langmead, B., Trapnell, C., Pop, M., and Salzberg, S.L. (2009). Ultrafast and memory-efficient alignment of short DNA sequences to the human genome. Genome Biol 10: R25.

Pubmed: [Author and Title](#)

CrossRef: [Author and Title](#)

Google Scholar: [Author Only](#) [Title Only](#) [Author and Title](#)

Laugesen, A. and Helin, K. (2014). Chromatin repressive complexes in stem cells, development, and cancer. Cell Stem Cell 14: 735-751.

Pubmed: [Author and Title](#)

CrossRef: [Author and Title](#)

Google Scholar: [Author Only](#) [Title Only](#) [Author and Title](#)

Lee, J.-Y., Colinas, J., Wang, J.Y., Mace, D., Ohler, U., and Benfey, P.N. (2006). Transcriptional and posttranscriptional regulation of transcription factor expression in Arabidopsis roots. Proc. Natl. Acad. Sci. U.S.A. 103: 6055-6060.

Pubmed: [Author and Title](#)

CrossRef: [Author and Title](#)

Google Scholar: [Author Only](#) [Title Only](#) [Author and Title](#)

Ma, S., Shah, S., Bohnert, H.J., Snyder, M., and Dinesh-Kumar, S.P. (2013). Incorporating motif analysis into gene co-expression networks reveals novel modular expression pattern and new signaling pathways. PLoS Genet 9: e1003840.

Pubmed: [Author and Title](#)

CrossRef: [Author and Title](#)

Google Scholar: [Author Only](#) [Title Only](#) [Author and Title](#)

Mahonen, A.P. (2000). A novel two-component hybrid molecule regulates vascular morphogenesis of the Arabidopsis root. Genes & Development 14: 2938-2943.

Pubmed: [Author and Title](#)

CrossRef: [Author and Title](#)

Google Scholar: [Author Only](#) [Title Only](#) [Author and Title](#)

Mahonen, A.P. (2006). Cytokinin Signaling and Its Inhibitor AHP6 Regulate Cell Fate During Vascular Development. Science 311: 94-98.

Pubmed: [Author and Title](#)

CrossRef: [Author and Title](#)

Google Scholar: [Author Only](#) [Title Only](#) [Author and Title](#)

Mallory, A.C. (2005). MicroRNA-Directed Regulation of Arabidopsis AUXIN RESPONSE FACTOR17 Is Essential for Proper Development and Modulates Expression of Early Auxin Response Genes. THE PLANT CELL ONLINE 17: 1360-1375.

Pubmed: [Author and Title](#)

CrossRef: [Author and Title](#)

Google Scholar: [Author Only](#) [Title Only](#) [Author and Title](#)

Margueron, R. and Reinberg, D. (2011). The Polycomb complex PRC2 and its mark in life. Nature 469: 343-349.

Pubmed: [Author and Title](#)
CrossRef: [Author and Title](#)
Google Scholar: [Author Only](#) [Title Only](#) [Author and Title](#)

Margueron, R., Li, G., Sarma, K., Blais, A., Zavadil, J., Woodcock, C.L., Dynlacht, B.D., and Reinberg, D. (2008). Ezh1 and Ezh2 maintain repressive chromatin through different mechanisms. *Molecular Cell* 32: 503-518.

Pubmed: [Author and Title](#)
CrossRef: [Author and Title](#)
Google Scholar: [Author Only](#) [Title Only](#) [Author and Title](#)

Mozgová, I. and Hennig, L. (2015). The Polycomb Group Protein Regulatory Network. <http://dx.doi.org/10.1146/annurev-arplant-043014-115627>.

Pubmed: [Author and Title](#)
CrossRef: [Author and Title](#)
Google Scholar: [Author Only](#) [Title Only](#) [Author and Title](#)

Nakagawa, T., Kurose, T., Hino, T., Tanaka, K., Kawamukai, M., Niwa, Y., Toyooka, K., Matsuoka, K., Jinbo, T., and Kimura, T. (2007). Development of series of gateway binary vectors, pGWBs, for realizing efficient construction of fusion genes for plant transformation. *J. Biosci. Bioeng.* 104: 34-41.

Pubmed: [Author and Title](#)
CrossRef: [Author and Title](#)
Google Scholar: [Author Only](#) [Title Only](#) [Author and Title](#)

Ohno, K., McCabe, D., Czermin, B., Imhof, A., and Pirrotta, V. (2008). ESC, ESCL and their roles in Polycomb Group mechanisms. *Mech. Dev.* 125: 527-541.

Pubmed: [Author and Title](#)
CrossRef: [Author and Title](#)
Google Scholar: [Author Only](#) [Title Only](#) [Author and Title](#)

Okushima, Y. (2005). Functional Genomic Analysis of the AUXIN RESPONSE FACTOR Gene Family Members in *Arabidopsis thaliana*: Unique and Overlapping Functions of ARF7 and ARF19. *The Plant Cell* 17: 444-463.

Pubmed: [Author and Title](#)
CrossRef: [Author and Title](#)
Google Scholar: [Author Only](#) [Title Only](#) [Author and Title](#)

Ossowski, S., Schwab, R., and Weigel, D. (2008). Gene silencing in plants using artificial microRNAs and other small RNAs. *The Plant Journal* 53: 674-690.

Pubmed: [Author and Title](#)
CrossRef: [Author and Title](#)
Google Scholar: [Author Only](#) [Title Only](#) [Author and Title](#)

Pasini, D., Bracken, AP., Hansen, J.B., Capillo, M., and Helin, K. (2007). The polycomb group protein Suz12 is required for embryonic stem cell differentiation. *Mol. Cell. Biol.* 27: 3769-3779.

Pubmed: [Author and Title](#)
CrossRef: [Author and Title](#)
Google Scholar: [Author Only](#) [Title Only](#) [Author and Title](#)

Quinlan, AR. and Hall, I.M. (2010). BEDTools: a flexible suite of utilities for comparing genomic features. *Bioinformatics* 26: 841-842.

Pubmed: [Author and Title](#)
CrossRef: [Author and Title](#)
Google Scholar: [Author Only](#) [Title Only](#) [Author and Title](#)

Rademacher, E.H., Möller, B., Lokerse, AS., Llavata-Peris, C.I., van den Berg, W., and Weijers, D. (2011). A cellular expression map of the *Arabidopsis* AUXIN RESPONSE FACTOR gene family. *The Plant Journal* 68: 597-606.

Pubmed: [Author and Title](#)
CrossRef: [Author and Title](#)
Google Scholar: [Author Only](#) [Title Only](#) [Author and Title](#)

Reece-Hoyes, J.S. et al. (2011). Yeast one-hybrid assays for gene-centered human gene regulatory network mapping. *Nat Meth* 8: 1050-1052.

Pubmed: [Author and Title](#)
CrossRef: [Author and Title](#)
Google Scholar: [Author Only](#) [Title Only](#) [Author and Title](#)

Roudier, F. et al. (2011). Integrative epigenomic mapping defines four main chromatin states in *Arabidopsis*. *The EMBO Journal* 30: 1928-1938.

Pubmed: [Author and Title](#)
CrossRef: [Author and Title](#)
Google Scholar: [Author Only](#) [Title Only](#) [Author and Title](#)

Rueda-Romero, P., Barrero-Sicilia, C., Gómez-Cadenas, A., Carbonero, P., and Oñate-Sánchez, L. (2012). *Arabidopsis thaliana* DOF6 negatively affects germination in non-after-ripened seeds and interacts with TCP14. *Journal of Experimental Botany* 63: 1937-1949.

Pubmed: [Author and Title](#)
CrossRef: [Author and Title](#)
Google Scholar: [Author Only](#) [Title Only](#) [Author and Title](#)

Scheres, B. (2007). Stem-cell niches: nursery rhymes across kingdoms. *Nature Reviews Molecular Cell Biology* 8: 345-354.

Pubmed: [Author and Title](#)

CrossRef: [Author and Title](#)
Google Scholar: [Author Only Title Only Author and Title](#)

Shahram Emami, M.-C.Y.J.R.D. (2013). A robust family of Golden Gate Agrobacterium vectors for plant synthetic biology. Front Plant Sci 4.

Pubmed: [Author and Title](#)
CrossRef: [Author and Title](#)
Google Scholar: [Author Only Title Only Author and Title](#)

Shannon, P., Markiel, A, Ozier, O., Baliga, N.S., Wang, J.T., Ramage, D., Amin, N., Schwikowski, B., and Ideker, T. (2003). Cytoscape: a software environment for integrated models of biomolecular interaction networks. Genome Research 13: 2498-2504.

Pubmed: [Author and Title](#)
CrossRef: [Author and Title](#)
Google Scholar: [Author Only Title Only Author and Title](#)

She, W., Grimanelli, D., and Baroux, C. (2014). An efficient method for quantitative, single-cell analysis of chromatin modification and nuclear architecture in whole-mount ovules in Arabidopsis. J Vis Exp: e51530.

Pubmed: [Author and Title](#)
CrossRef: [Author and Title](#)
Google Scholar: [Author Only Title Only Author and Title](#)

Sher, F., Rössler, R., Brouwer, N., Balasubramaniyan, V., Boddeke, E., and Copray, S. (2008). Differentiation of neural stem cells into oligodendrocytes: involvement of the polycomb group protein Ezh2. Stem Cells 26: 2875-2883.

Pubmed: [Author and Title](#)
CrossRef: [Author and Title](#)
Google Scholar: [Author Only Title Only Author and Title](#)

Sieburth, L.E. and Meyerowitz, E.M. (1997). Molecular dissection of the AGAMOUS control region shows that cis elements for spatial regulation are located intragenically. The Plant Cell 9: 355-365.

Pubmed: [Author and Title](#)
CrossRef: [Author and Title](#)
Google Scholar: [Author Only Title Only Author and Title](#)

Stojic, L. et al. (2011). Chromatin regulated interchange between polycomb repressive complex 2 (PRC2)-Ezh2 and PRC2-Ezh1 complexes controls myogenin activation in skeletal muscle cells. Epigenetics Chromatin 4: 16.

Pubmed: [Author and Title](#)
CrossRef: [Author and Title](#)
Google Scholar: [Author Only Title Only Author and Title](#)

Takawa, M. et al. (2011). Validation of the histone methyltransferase EZH2 as a therapeutic target for various types of human cancer and as a prognostic marker. Cancer Sci. 102: 1298-1305.

Pubmed: [Author and Title](#)
CrossRef: [Author and Title](#)
Google Scholar: [Author Only Title Only Author and Title](#)

Taylor-Teeple, M. et al. (2015). An Arabidopsis gene regulatory network for secondary cell wall synthesis. Nature 517: 571-575.

Pubmed: [Author and Title](#)
CrossRef: [Author and Title](#)
Google Scholar: [Author Only Title Only Author and Title](#)

Terpstra, I. and Heidstra, R. (2009). Stem cells: The root of all cells. Seminars in Cell & Developmental Biology 20: 1089-1096.

Pubmed: [Author and Title](#)
CrossRef: [Author and Title](#)
Google Scholar: [Author Only Title Only Author and Title](#)

Truernit, E., Bauby, H., Dubreucq, B., Grandjean, O., Runions, J., Barthelemy, J., and Palauqui, J.C. (2008). High-Resolution Whole-Mount Imaging of Three-Dimensional Tissue Organization and Gene Expression Enables the Study of Phloem Development and Structure in Arabidopsis. THE PLANT CELL ONLINE 20: 1494-1503.

Pubmed: [Author and Title](#)
CrossRef: [Author and Title](#)
Google Scholar: [Author Only Title Only Author and Title](#)

Turck, F., Roudier, F., Farrona, S., Martin-Magniette, M.-L., Guillaume, E., Buisine, N., Gagnot, S., Martienssen, R.A., Coupland, G., and Colot, V. (2007). Arabidopsis TFL2/LHP1 specifically associates with genes marked by trimethylation of histone H3 lysine 27. PLoS Genet 3: e86.

Pubmed: [Author and Title](#)
CrossRef: [Author and Title](#)
Google Scholar: [Author Only Title Only Author and Title](#)

Varambally, S., Dhanasekaran, S.M., Zhou, M., Barrette, T.R., Kumar-Sinha, C., Sanda, M.G., Ghosh, D., Pienta, K.J., Sewalt, R.G.A.B., Otte, A.P., Rubin, M.A., and Chinnaiyan, A.M. (2002). The polycomb group protein EZH2 is involved in progression of prostate cancer. Nature 419: 624-629.

Pubmed: [Author and Title](#)
CrossRef: [Author and Title](#)
Google Scholar: [Author Only Title Only Author and Title](#)

Wagener, N., Macher-Goeppinger, S., Pritsch, M., Hüsing, J., Hoppe-Seyler, K., Schirmacher, P., Pfitzenmaier, J., Haferkamp, A., Hoppe-Seyler, F., and Hohenfellner, M. (2010). Enhancer of zeste homolog 2 (EZH2) expression is an independent prognostic factor in renal cell carcinoma. BMC Cancer 10: 524.

Pubmed: [Author and Title](#)

CrossRef: [Author and Title](#)
Google Scholar: [Author Only Title Only Author and Title](#)

Wang, D., Tyson, M.D., Jackson, S.S., and Yadegari, R. (2006). Partially redundant functions of two SET-domain polycomb-group proteins in controlling initiation of seed development in Arabidopsis. Proc. Natl. Acad. Sci. U.S.A 103: 13244-13249.

Pubmed: [Author and Title](#)
CrossRef: [Author and Title](#)
Google Scholar: [Author Only Title Only Author and Title](#)

Yadegari, R., Kinoshita, T., Lotan, O., Cohen, G., Katz, A., Choi, Y., Katz, A., Nakashima, K., Harada, J.J., Goldberg, R.B., Fischer, R.L., and Ohad, N. (2000). Mutations in the FIE and MEA genes that encode interacting polycomb proteins cause parent-of-origin effects on seed development by distinct mechanisms. The Plant Cell 12: 2367-2382.

Pubmed: [Author and Title](#)
CrossRef: [Author and Title](#)
Google Scholar: [Author Only Title Only Author and Title](#)

Yamaguchi, M., Ohtani, M., Mitsuda, N., Kubo, M., Ohme-Takagi, M., Fukuda, H., and Demura, T. (2010). VND-INTERACTING2, a NAC domain transcription factor, negatively regulates xylem vessel formation in Arabidopsis. THE PLANT CELL ONLINE 22: 1249-1263.

Pubmed: [Author and Title](#)
CrossRef: [Author and Title](#)
Google Scholar: [Author Only Title Only Author and Title](#)

Zhang, X., Clarenz, O., Cokus, S., Bernatavichute, Y.V., Pellegrini, M., Goodrich, J., and Jacobsen, S.E. (2007a). Whole-genome analysis of histone H3 lysine 27 trimethylation in Arabidopsis. Plos Biol 5: e129.

Pubmed: [Author and Title](#)
CrossRef: [Author and Title](#)
Google Scholar: [Author Only Title Only Author and Title](#)

Zhang, X., Germann, S., Blus, B.J., Khorasanizadeh, S., Gaudin, V., and Jacobsen, S.E. (2007b). The Arabidopsis LHP1 protein colocalizes with histone H3 Lys27 trimethylation. Nat. Struct. Mol. Biol. 14: 869-871.

Pubmed: [Author and Title](#)
CrossRef: [Author and Title](#)
Google Scholar: [Author Only Title Only Author and Title](#)

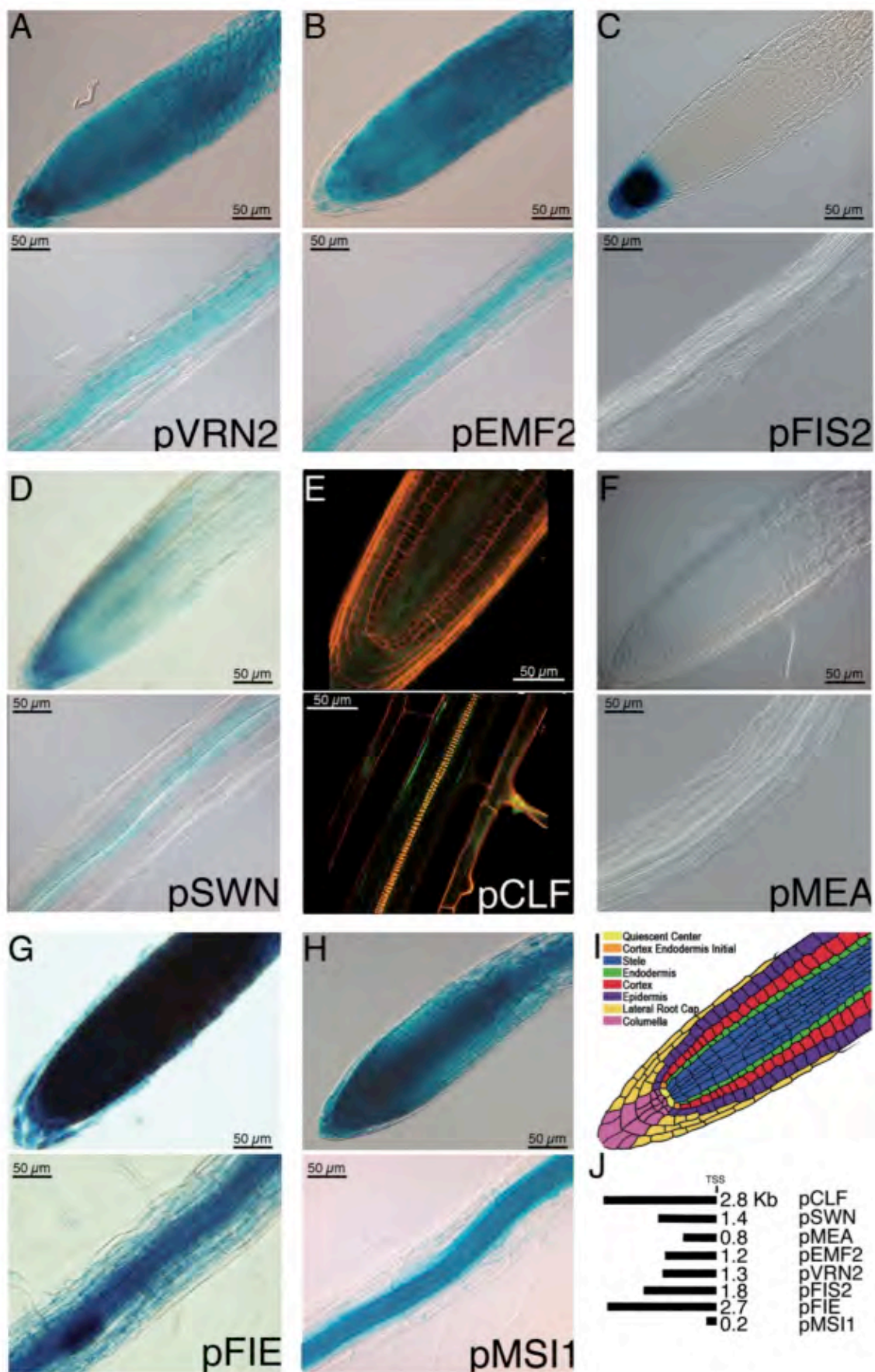


Figure 1. PRC2 genes are expressed in unique and overlapping cell types in the *Arabidopsis thaliana* root. For each genotype, the top panel shows the root meristem while the bottom panel shows the maturation/differentiation zone of the root. All images were taken under the same acquisition conditions. (A) VRN2pro:GUS expression. (B) EMF2pro:GUS expression. (C) FIS2pro:GUS expression. (D) SWNpro:GUS expression. (E) CLFpro:VenusN7 expression. (F) MEApr:GUS expression. (G) FIEpro:GUS expression. (H) MSI1pro:GUS expression. (I) Cartoon of the different cell types and tissues in the *Arabidopsis thaliana* root. (J) Promoter lengths of the different PRC2 genes used in the reporter lines. Translational start site = TSS.

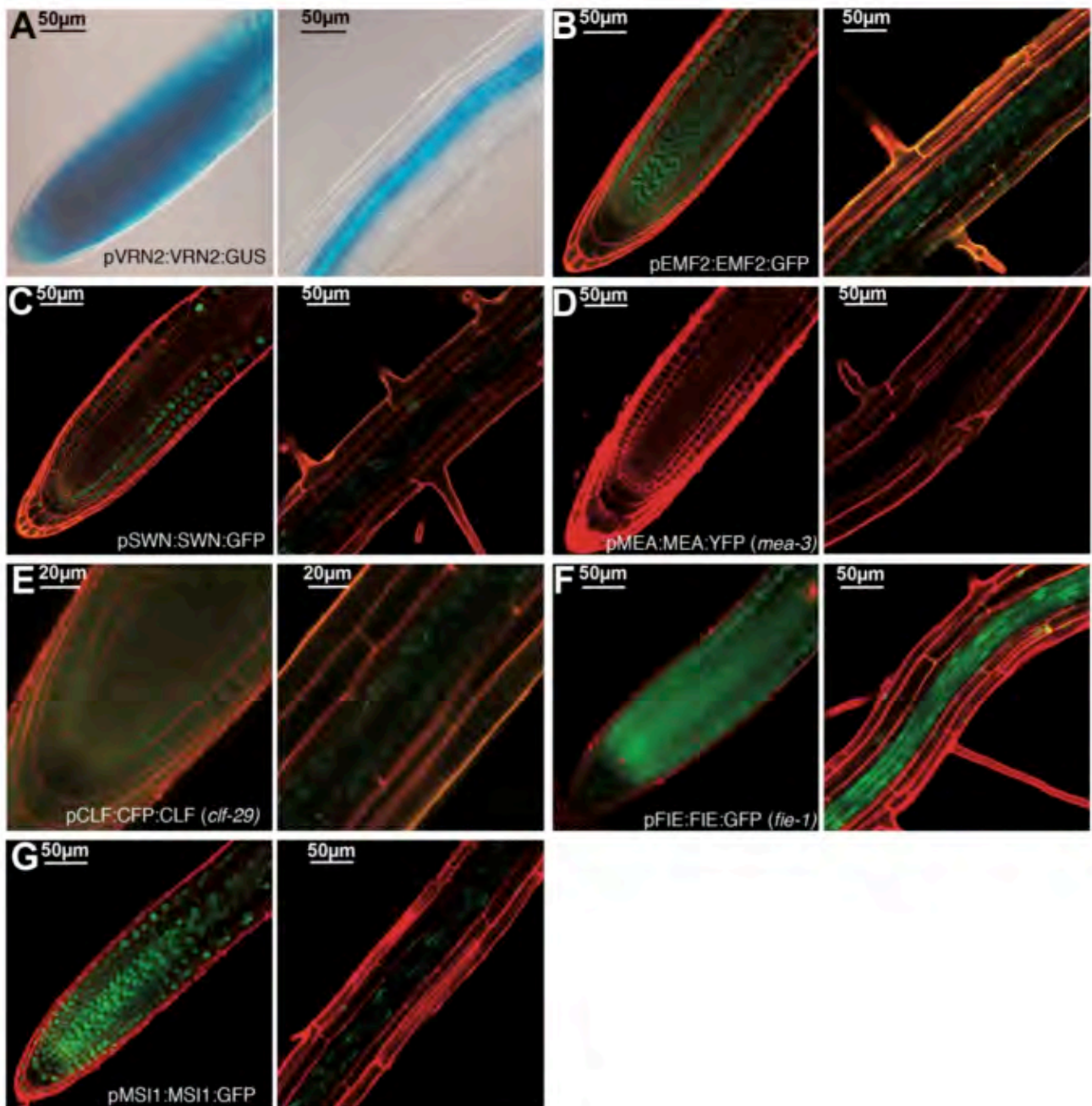


Figure 2: PRC2 proteins are found in unique and overlapping cell types in the *Arabidopsis thaliana* root. For each genotype, the left panel shows the root meristem while the right panel shows the maturation/differentiation zone of the root. (A) VRN2pro:VRN2:GUS (B) EMF2pro:EMF2:GFP (C) SWNpro:SWN:GFP (D) MEApr:MEA:YFP in *mea-3* (E) CLFpro:CFP:gCLF in *clf-29*, (F) MSI1pro:MSI1:GFP (G) FIEpro:FIE:GFP in *fie-1*.

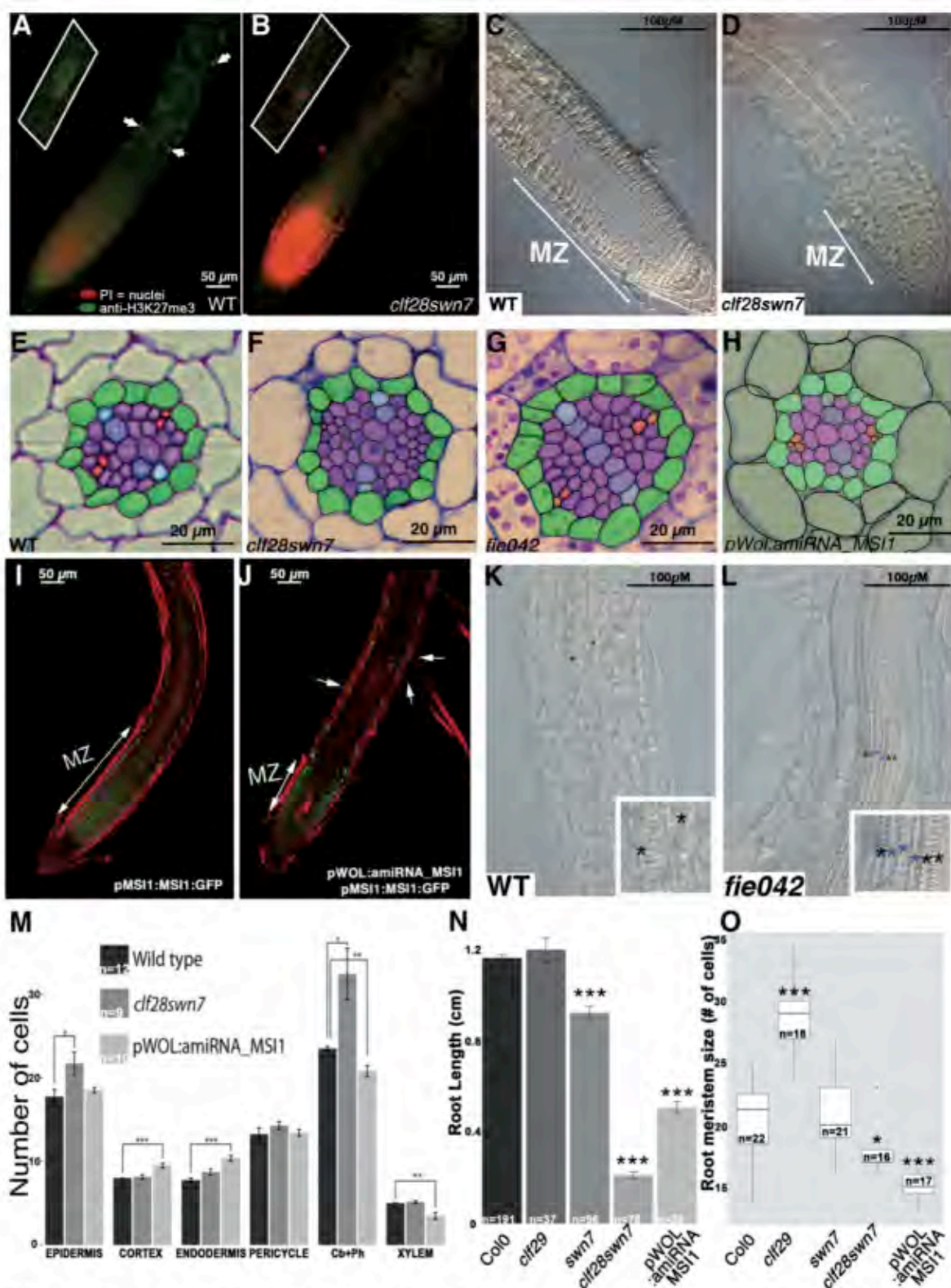


Figure 3: PRC2 regulates cell proliferation in the root meristem and vascular cylinder. (A-B) Whole mount immunostaining with antibodies specific for H3K27me3 (green in the wild-type Col-0) (A) and in the *clf-28 swn-7* double mutant (B). Nuclear staining is indicated with white arrows. A magnified nucleus is shown in the inset. (C-D) Differential Interference Contrast image of the root meristem of the wild-type Col-0 (C) and the *clf-28 swn-7* double mutant (D). White lines indicate the root meristematic zone (MZ). (E-H) Cross-sections showing the root vascular cylinder in wild-type Col-0 (E), *clf-28 swn-7* (F), *fie042* (G), and in the WOLpro:amiRNA_MSI line (H). Green indicates pericycle cells, purple indicates procambium cells, red/orange indicates phloem cells. (I-J) The MSI protein is expressed ubiquitously throughout the *Arabidopsis thaliana* root (I) but is depleted specifically from the vascular cylinder in the WOLpro:amiRNA_MSI1 line in the MSI1pro:MSI1:GFP background (white arrows with one head) (J). Note the reduction in the length of the root meristem (white arrow with two heads). (K-L) Differential interference contrast image showing two protoxylem pole cell files (black asterisk) in the wild-type Col-0 (L) and ectopic protoxylem (black asterisk) and metaxylem (blue asterisk) in the *fie042* mutant background (L). (M) There are significantly more procambium and phloem and epidermal cells in the *clf-28 swn-7* mutant compared to wild-type Col-0. The reduction in MSI1 expression shows increased number of cortical and endodermal cells but lower levels of cells in the stele. (N) The roots of *swn-7*, *clf-28 swn-7* and WOLpro:amiRNA_MSI are significantly shorter than wild type Col-0 and *clf-29*. (O) There are more cells in the meristem of *clf-29* and fewer in *clf-28 swn-7* and WOLpro:amiRNA_MSI relative to wild type (Col-0). In all cases, significance was tested using a t-test. * = $p < .05$; ** = $p < .01$; *** = $p < .001$. Error bars indicate the standard error value.

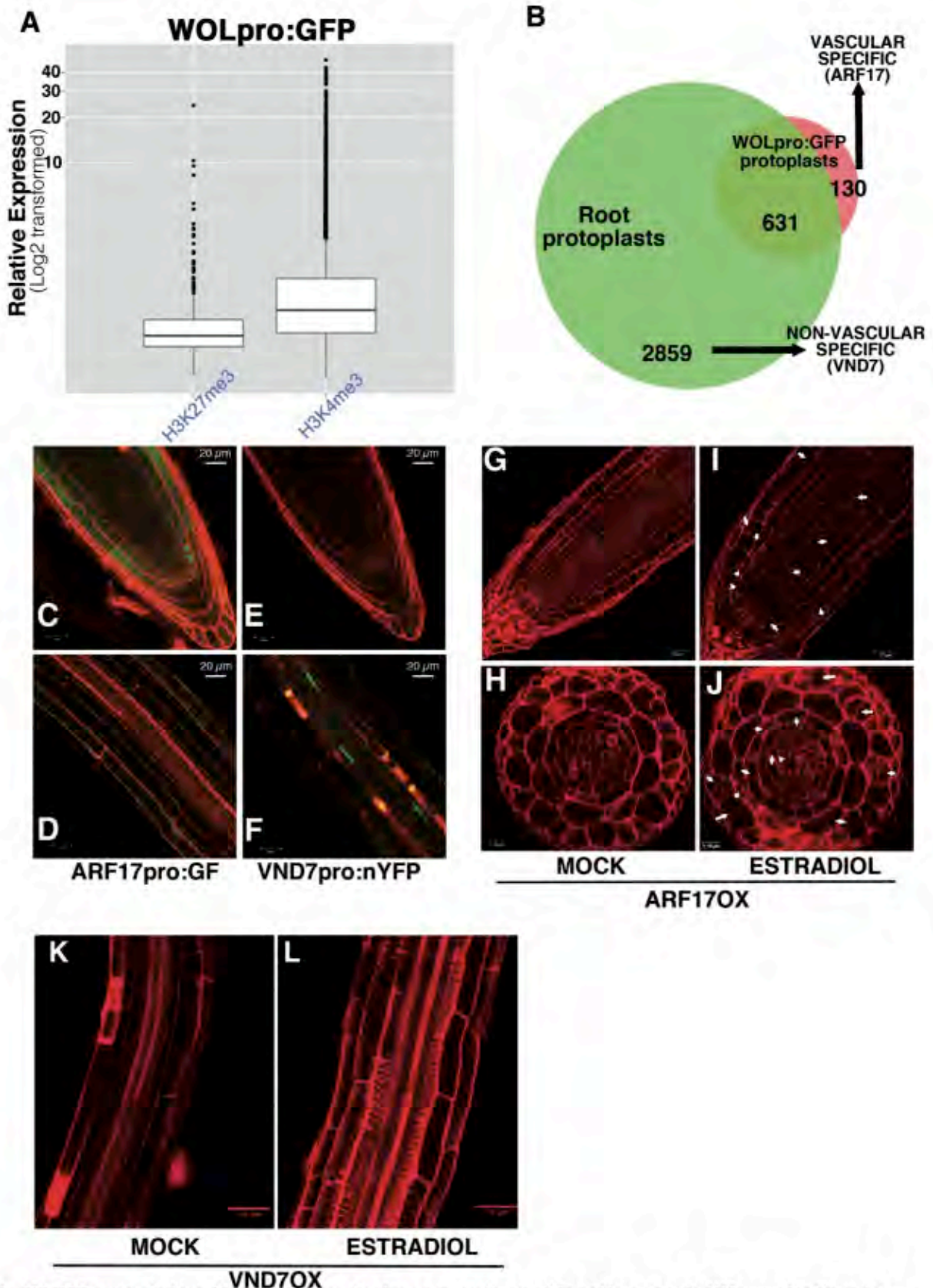


Figure 4. PRC2 regulates the balance between cell proliferation and differentiation in a tissue-specific manner in the *Arabidopsis thaliana* root. (A) Expression levels of genes marked by H3K27me3 in vascular cells relative to expression levels of genes marked by H3K4me3. Whole root and vascular-specific (pWOL:GFP positive) root protoplast were isolated by FACS and H3K27me3/H3K4me3 enriched regions were resolved by ChIPseq. Expression of the vascular specific H3K27me3 and H3K4me3 marked genes was determined using Brady et. al. 2007 transcriptional data. (B) Number of genes marked by H3K27me3 in non-vascular cells. (C-F) Expression of a gene marked specifically by H3K27me3 and not expressed in vascular cells (C,D) ARF17pro:GF and of a gene marked specifically by H3K27me3 and not expressed in non-vascular cells VND7pro:nYFP (E,F). (G-J) Estradiol induction of the ARF17 transcription factor results in small regions of additional cell proliferation in the vascular cylinder (I,J) compared to the mock-treated root (G,H). Asterisks indicate ectopic cell proliferation. (K-L) Estradiol induction of the VND7 transcription factor (L) results in ectopic xylem cell differentiation compared to a mock-treated root (K).

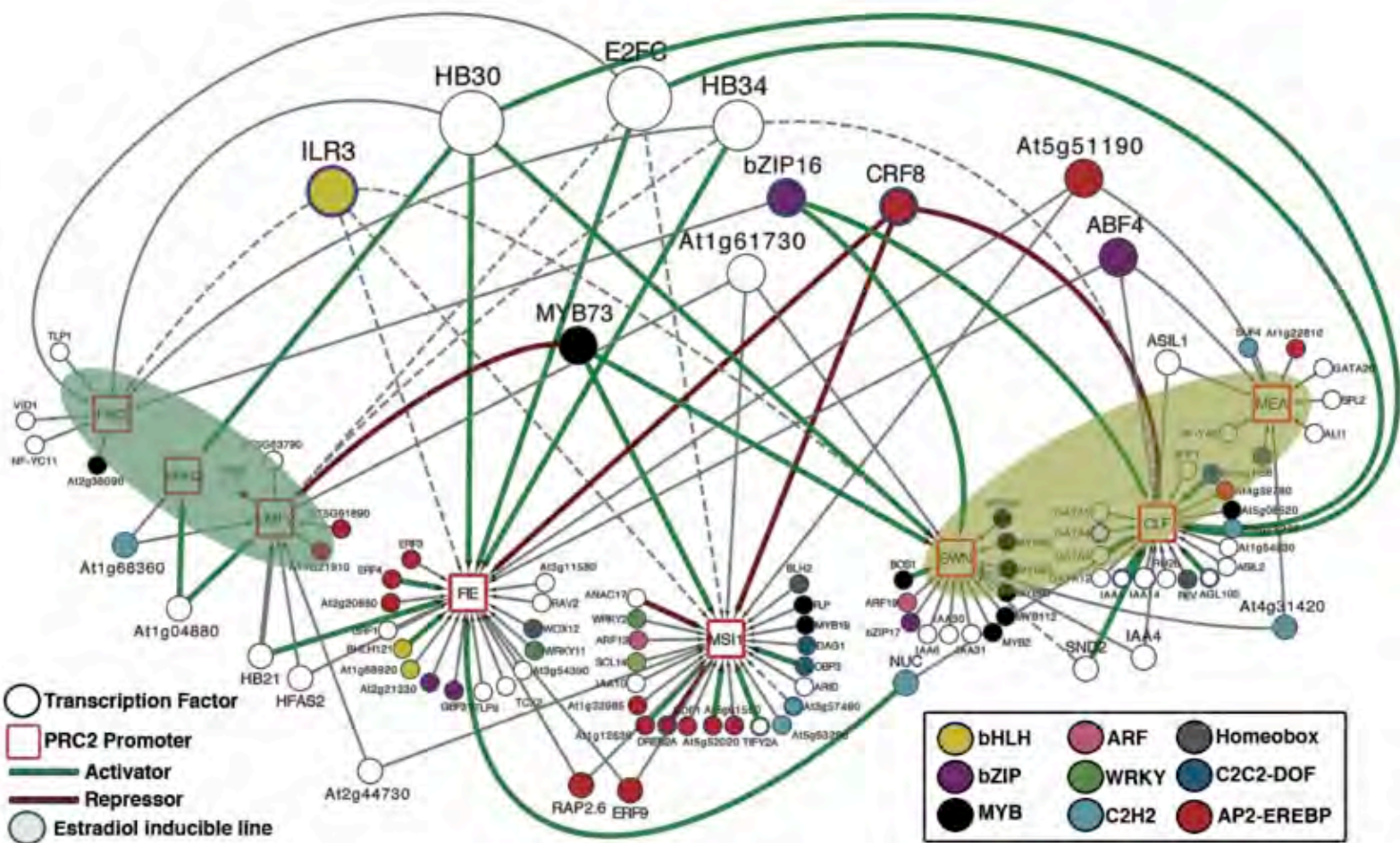


Figure 5. Transcription factors regulating PRC2 gene expression in planta. Squares represent PRC2 gene promoters, circles represent transcription factors. A line between a transcription factor and promoter indicates that an interaction was observed by yeast one hybrid. A green line or a red line indicates that the transcription factor has been validated in planta as activating or repressing, respectively, the target gene in planta in either a trans-activation assay or upon B-estradiol induction of the transcription factor. Transcription factors are additionally colored according to their respective family. Transcription factors that interact with the most PRC2 gene promoters are indicated at the top of the network, while transcription factors that interact with just a single promoter are located just beside their respective PRC2 gene promoter.

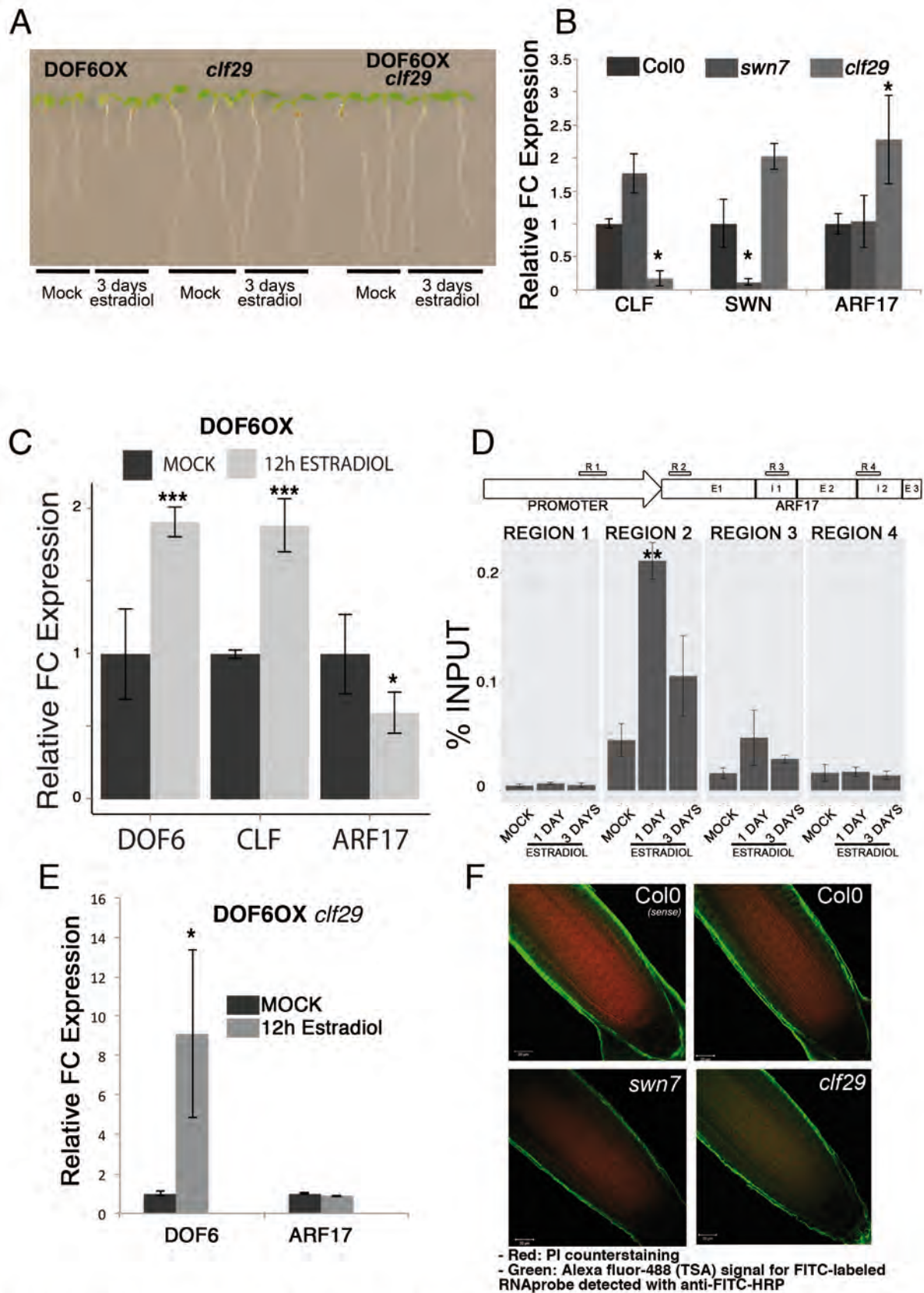


Figure 6. Functional validation of a multi-tier PRC2 gene regulatory network (TF → PRC2 gene → H3K27me3 regulated gene). (A) β -estradiol induction (3 days) of the DOF6 transcription factor results in a significantly shorter root. Root inhibition caused by the induction of DOF6 is abolished in the *clf29* background. (B) ARF17 expression is activated in the *clf-29* mutant. (C) Induction of DOF6 results in a significant increase in the amount of CLF expression and a corresponding repression of ARF17 expression, as revealed by RT-qPCR. (D) Induction of DOF6 results in a significant increase in H3K27me3 deposition in the ARF17 loci in the root tissue. (E) DOF6 induction does not affect ARF17 expression in the *clf-29* background. (F) Whole mount in-situ hybridization of ARF17 mRNA. ARF17 expression domain is expanded towards the vascular cylinder in the *clf-29* mutant. In all cases significance was tested using a t-test. * = $p < .05$; ** = $p < .01$; *** = $p < .001$. Error bars represent the standard error value of the log2 transformed expression. The mean is from 3 independent experiments (biological replicates), calculated from the average of 3 technical replicates per biological replicate. Each biological replicate captures expression from approximately 200 roots of each respective genotype. In each case the $\Delta\Delta Ct$ was calculated relative to an ubiquitin10 control.

Transcriptional Regulation of Arabidopsis Polycomb Repressive Complex 2 Coordinates Cell Type Proliferation and Differentiation

Miguel de Lucas, Li Pu, Gina Marie Turco, Allie Gaudinier, Ana Karina Marao, Hirofumi Harashima, Dahae Kim, Mily Ron, Keiko Sugimoto, Francois M Roudier and Siobhan M. Brady
Plant Cell; originally published online September 20, 2016;
DOI 10.1105/tpc.15.00744

This information is current as of September 25, 2016

Supplemental Data	http://www.plantcell.org/content/suppl/2016/09/20/tpc.15.00744.DC1.html
Permissions	https://www.copyright.com/ccc/openurl.do?sid=pd_hw1532298X&issn=1532298X&WT.mc_id=pd_hw1532298X
eTOCs	Sign up for eTOCs at: http://www.plantcell.org/cgi/alerts/ctmain
CiteTrack Alerts	Sign up for CiteTrack Alerts at: http://www.plantcell.org/cgi/alerts/ctmain
Subscription Information	Subscription Information for <i>The Plant Cell</i> and <i>Plant Physiology</i> is available at: http://www.aspb.org/publications/subscriptions.cfm